Mathematical Biosciences and Engineering

MBE, 22(2): 431–476.
DOI: 10.3934/mbe.2025017
Received: 26 September 2024
Revised: 18 December 2024
Accepted: 02 January 2025
Published: 13 February 2025

http://www.aimspress.com/journal/MBE

Review

Computational modeling of peritoneal dialysis: An overview

Sangita Swapnasrita[1,2], Joost C de Vries[2], Carl M. Öberg[3], Aurélie MF Carlier[1,*] and Karin GF Gerritsen[2,*]

[1] MERLN Institute for Regenerative Medicine, Maastricht University, Universiteitssingel 40, 6229 ER Maastricht, The Netherlands
[2] Department of Nephrology and Hypertension, University Medical Center Utrecht, Heidelberglaan 100, 3584 CX Utrecht, The Netherlands
[3] Department of Clinical Sciences Lund, Division of Nephrology, Skåne University Hospital, Lund, University, Lund, Sweden

* **Correspondence:** Email: K.G.F.Gerritsen@umcutrecht.nl, a.carlier@maastrichtuniversity.nl.

Abstract: Peritoneal dialysis (PD) is a kidney replacement therapy for patients with end-stage renal disease. It is becoming more popular as a result of a rising interest in home dialysis. Its effectiveness depends on several physiological and technical factors, which have led to the development of various computational models to better understand and predict PD outcomes. In this review, we traced the evolution of computational PD models, discussed the principles underlying these models, including the transport kinetics of solutes, the fluid dynamics within the peritoneal cavity, and the peritoneal membrane properties, and reviewed the various PD models that can be used to optimize and personalize PD treatment. By providing a comprehensive overview, we aim to guide both current clinical practice and future research into novel PD techniques such as the application of continuous flow and sorbent-based dialysate regeneration where mathematical modeling may offer an inexpensive and effective tool to optimize design of these novel techniques at a patient specific level.

Keywords: peritoneal dialysis; mathematical modeling; solute flux; volume flux; parameter determination

1. Peritoneal dialysis

Over 850 million people worldwide, i.e., ~1 in every 10, suffer to some degree from chronic kidney disease [1], among which over 3.8 million are on dialysis, either peritoneal dialysis (PD) or hemodialysis (HD) [2]. During PD, dialysis fluid is instilled into the abdominal cavity via a permanent catheter. The lining of the abdominal cavity (the peritoneum) acts as a semi-permeable membrane for solute and water transport. PD removes waste products from blood plasma by diffusion and convection across the peritoneal membrane into the dialysis fluid in the abdominal cavity (see Figure 1). Excess water is removed via osmosis using glucose or -less commonly- amino acids as crystalloid osmotic agents in the dialysis fluid and icodextrin, a mixture of glucose polymers, as colloid osmotic agent [3,4]. While glucose and amino acids are rapidly absorbed across the peritoneal membranes, icodextrin is absorbed only to a limited extent due to its large molecular weight (on average 12–20 kDa [5]) exerting a sustained osmotic effect suitable for sustained fluid removal during longer dwell times [3,6]. Three types of pores are distinguished to properly describe solute and fluid transport across the peritoneal membrane: Small pores, which facilitate small solute transport; large pores, which are responsible for movement of larger solutes such as proteins; and ultra-small pores, which enable the passage of water molecules [7]. Selective water transport through the latter is responsible for an initial decrease in dialysate sodium concentration during the early dwell phase and it may explain glucose's osmotic efficacy despite its high diffusibility. Continuous ambulatory PD (CAPD) and automated PD (APD) are the two major modalities of PD used in routine practice. With CAPD, the dialysis fluid (1–2.5 L) is exchanged (drained and instilled) 3–4 times daily manually through the catheter [8]. During daytime, glucose-based solutions are typically used with dwells lasting 4–6 hours. During the night, a long dwell with an icodextrin solution is commonly used. With APD, a cycler with patient specific treatment parameters is connected to the abdominal catheter throughout the session (preferably at night) to automatically perform exchanges with (glucose-based) dialysis fluid over a period of time (usually 4–5 per night) [9]. This is often combined with a long dwell with an icodextrin solution (14–15 h) during the day. Both CAPD and APD are usually conducted every day of the week.

PD has several advantages compared to HD: it enables continuous gradual removal of waste (instead of intermittent HD, which is characterized by a 'saw-tooth pattern'), does not require blood access, provides more patient autonomy as the treatment is performed at home, and is less expensive. Residual kidney function is also better preserved [10] compared to HD. However, PD has important shortcomings. Technique survival is limited (median 3.7 years [11]) due to recurrent peritonitis (inflammation of the peritoneal membrane), catheter dysfunction or membrane failure (due to exposure to high (harmful) dialysate glucose concentrations required for osmotic water removal), and small solute clearance is relatively low. Due to technique failure or low small solute clearance (with disappearance of residual diuresis) patients often have to switch to HD after several years [11,12].

Despite 60 years of progress in PD, it is used only by ~11% of dialysis patients with considerable variations across countries, mostly due to non-medical reasons [13–15]. Strikingly, Hong Kong has ~80% end stage kidney disease (ESKD) patients on PD to reduce expenditure [16] after an implementation of "PD first" policies. Mexico, Thailand, and Singapore also have high rates of PD due to availability of medical personnel to assist with PD. To increase PD usage, improve outcomes, and better personalize PD regimens, there are several novel techniques under development such as in

home production of peritoneal dialysate [13], novel PD solutions with improved biocompatibility and/or glucose-sparing, continuous flow PD [17,18], and sorbent assisted PD [19–21] (Figure 1). Glucose-sparing strategies include the use of alternative osmotic ingredients such as (commercially available) icodextrin and amino acids or alternatives that are under development such as taurine, polyglycerol, carnitine, xylitol, and alanyl-glutamine [3,22]. Moreover, combinations of crystalloid and colloid osmosis (so-called bi-modal osmosis) have been explored by mixing glucose with icodextrin, This approach leverages rapid initial ultrafiltration provided by glucose and sustained ultrafiltration by icodextrin and was shown to enhance fluid removal while reducing overall glucose exposure [4,23]. A study by Stachowska-Pietka et al. showed that comparing glucose 2.27% and icodextrin 7.5% in a patient group with average transfer rate, there was a 204% increase in ultrafiltration, 3.6% increase in glucose and carbohydrates absorbed, 163% increase in sodium removal, 13% increase in urea removal, and 17% increase in creatinine removal [6]. However, potential consequences are accumulation of icodextrin metabolites. In addition, using icodextrin and bimodal solutions increases the sodium removal leading to hyponatremia [24]. Since icodextrin modeling is relatively new, it has been briefly included in Sections 4 and 5 but has not been discussed extensively in this review.

In continuous flow PD (CFPD), there is a continuous flow of dialysate through an inflow catheter and outflow catheter [17,18,25]. The continuous flow of fresh dialysate through the abdominal cavity maintains a large plasma–dialysate concentration gradient, increasing solute transfer across the peritoneal membrane. Dialysate glucose concentration can be kept nearly constant, thereby maintaining a constant osmotic gradient and ultrafiltration rate at lower (peak) glucose concentrations than in conventional PD [26], possibly slowing functional deterioration of the peritoneal membrane and reducing the rate of peritonitis (both associated with high glucose concentrations). Sorbent-assisted PD regenerates the dialysis fluid using a sorbent cartridge [19,27,28].

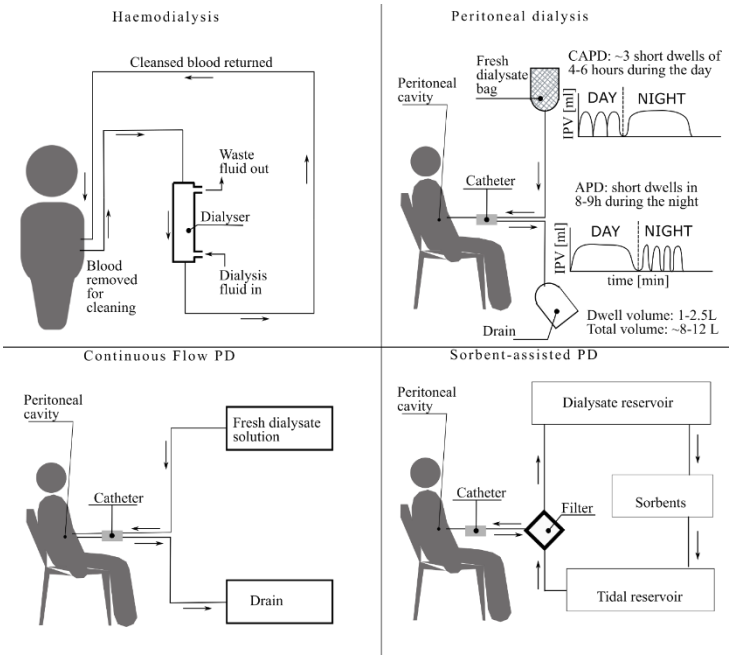

Figure 1. Different modes of dialysis therapy techniques available for the chronic kidney patient. IPV = Intraperitoneal volume.

The development of new technologies often takes a considerable amount of time owing to the learning curve, ensuring transparency, ethical requirements, trial regulations *et cetera* [29]. The new (post-2020) European Union Medical Device Regulation (EU-MDR) rules related to manufacturing of medical devices are more stringent, leading to delays in certification. As such, there is a need to supplement the pre-clinical research and clinical trials with other methodologies to accelerate the design and manufacture and market novel PD technologies. Computational models are a revolutionary tool in the field of health, medicine, and life sciences due to the ease of optimization, non-intrusiveness, and most importantly, the interpretation of complex interdependent physical processes. They are being increasingly used to study the influence of biological processes in medical devices, including, for example, thrombogenic reaction to biomaterials [30], controlled drug release [31], and effect of implant surface roughness on protein adsorption [32]. Computational modeling of PD may help clinicians make informed decisions, such as those involving catheter placement and treatment optimization [33,34]. Moreover, computational modeling is often an inexpensive and effective way to simulate complex natural phenomena.

In this review, we focus on computational models for PD, especially ordinary differential equation (ODE) models. ODE models represent homogeneous well-mixed compartmental systems that describe the evolution of the (solute) concentrations over time in the various compartments. In contrast, PDE models capture systems that are not well-mixed (accounting for catheter obstructions, recirculation, etc.), enabling the solute concentrations to be defined as a function of both time and space. As PDE models are beyond the scope of this discussion, they will not be addressed here. We follow the history of PD modeling to highlight the advances and remaining lacunas as well as learn which level of simplicity and physiological detail is necessary to reach a research aim. This review, containing general concepts of PD models, is specifically intended for experimental scientists or clinicians with little or no computational modeling experience, but who are interested in introducing modeling into their research practice. By providing an overview of computational models, the individual aspects of the models, and the scope of the model, we aim to simplify, enhance, and accelerate the integration of modeling into clinical practice to promote better understanding of device-patient interaction. In Section 6, we show an example of a scenario to illustrate how one can set up a mathematical model of PD using the models highlighted in this review.

2. Compartmental models for peritoneal dialysis

There are many types of computational models, including linear and non-linear, deterministic and stochastic, discrete and continuous and spatial and non-spatial ones. For general reviews on computational modeling we refer to Yates et al. [35], King et al. [36], and Brown et al. [37]. The most common design for models of PD is the compartmental model. They are simple in nature for physiological, kinetic and dynamic modeling. In compartmental models, the body is divided into theoretical compartments such as the peritoneal membrane, peritoneal cavity, and total body water (examples in Figure 2). The general assumption is that a tissue or organ can be represented as a homogeneous compartment, governed by conservation of mass and other properties of interest (e.g., charge). A compartmental model consists of volumes connected by fluxes of some entity. Each compartment can be a volume representation (in case of PD) and it characterizes the essential physics

and chemistry of the biological environment. The flow rates and interactions between the compartments are described by the parameters of the compartmental model. Some PD models use a single compartment model with just the peritoneal cavity and body considered to be a constant source of solutes [38] while some models include multiple compartments (e.g., the distributed model, [39]), with the peritoneal tissue, peritoneal cavity, and interstitium as different compartments. Compartment models are lumped models but despite their simplicity, they usually capture the underlying physical and biological phenomena quite well, which is why they are commonly used for PD modeling.

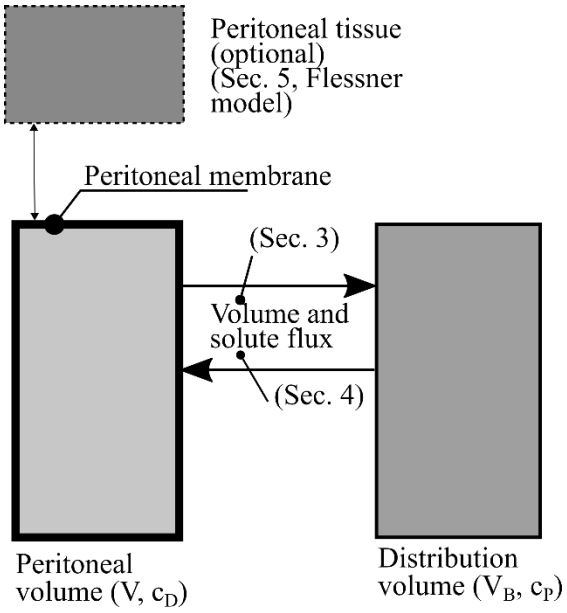

Figure 2. Compartmental PD modeling showing compartments (optional compartments in dotted lines), membranes, and fluxes. V = peritoneal compartment volume, V_B = Body compartment volume, and c_D and c_B = peritoneal and body solute concentration.

The models usually employ fluid and solute mass balance equations, which are described in Sections 3 and 4. This depends on the type of fluid flow (static or continuous), complexity (single compartment or distributed), and membrane model (continuous semi-permeable membrane or 3 pore) to decide which and how the fluid and solute flows should be properly modeled. In case of PD, physiologically, the barrier is a semi-permeable peritoneal membrane. The compartments can exchange the fluid and solutes without any barrier or with a barrier.

The simplest interpretation of the peritoneal membrane is a simple membrane that enables passive diffusion of solutes [40–42]. The diffusive flow of molecules (J_s in mol/s) will be dependent on the concentration gradient $\frac{dc}{dx}$ across the barrier:

$$J_s \propto \frac{dc}{dx} \tag{1}$$

$$J_s = -DA\frac{dc}{dx} \tag{2}$$

where D is the diffusion coefficient ($m^2\ s^{-1}$), A is the effective surface area available for diffusion (m^2), c is the concentration (mol/l), and x is the distance across the membrane (m). The negative sign is because the solute flux is in the opposite direction of the concentration gradient. Integrating the above equation (Eqs (1) and (2)) from $x = 0$ to $x = \Delta x$ (across the membrane),

$$J_s = -PS \cdot (c_2 - c_1) \tag{3}$$

where $PS = DA/\Delta x$, and c_1, c_2 are the concentrations on either side of the membrane, at $x = 0$ and $x = \Delta x$. c_1 and c_2 are usually chosen so that the sign of J_s is positive when transport is directed into the peritoneal cavity. Eq (3) can be used to calculate the diffusive plasma clearance of a particular solute from c_1 to c_2 (J_s/c_1) or vice versa (J_s/c_2). The factor PS is known as the diffusion capacity of the solute species and is defined as the maximal absolute diffusive plasma clearance (when the concentration is zero on one side of the membrane). Many abbreviations and terms are in use for this parameter such as mass transfer area coefficient (MTAC), k_{BD} etc.

2.1 Three-pore model of peritoneal dialysis

A perplexing thing about the peritoneal membrane is that it is a semi-permeable membrane that enables passage of albumin and other large proteins to a limited extent but also restricts the bulk movement of electrolytes [19,43–46]. In 1981, Nolph et al. stated, "It is a system that displays characteristics of some very large-pore radii when assessed by diffusion studies, and some very small-pore radii when assessed by ultrafiltration and solute reflection coefficients" [47]. The reflection coefficient, σ, describes the convective hindrance of a molecule (a value of 100% means convective clearance does not occur). Nolph et al. were the first to hypothesize that the peritoneal membrane is a heteroporous membrane with both small and large pores. Small pores with low solute permeability would be located in the proximal capillary and facilitate ultrafiltration due to the relatively high hydraulic pressure and high osmotic gradient in the proximal capillary. Toward the venous capillaries, the hydraulic pressure drops, and the oncotic pressure increases as a result of increased protein concentration caused by capillary ultrafiltration. A predominance of large "pores" in the venular capillaries with high permeability would facilitate diffusive solute exchange. Glucose would be more readily absorbed, resulting in lower osmotic pressure, and the ultrafiltration rate would be reduced at the venular capillaries also because of the relatively low hydrostatic and high oncotic pressure. In summary, most ultrafiltration would occur through the "small" pores with low hydraulic permeability and most solute exchange through highly permeable "large" pores (Figure 3A)). Aside from these two pathways, there is also a separate channel for movement of water that is inaccessible to solutes. To account for all three pathways, the three-pore model was developed.

In 1991 Rippe et al. [7] proposed the three pore model (Figure 3B)). This is the most common representation of the peritoneal membrane. It divides the body into two compartments – the distribution volume (specific to each solute) and the peritoneal cavity. The solute and volume flows through the

different pores that are defined by the Starling and Patlak equations, respectively (explained in Eqs (4) and (29)). The most abundant (99% of the pore fraction) is the protein restrictive water-soluble pathway (15 to 36 Å), which is responsible for 90% of the hydraulic conductance. The "large pores" of 250 Å constitute 0.01% of the pore population and represent 8% of the hydraulic conductance, and the final pore fraction is the ultrasmall pores (0.99%) and is responsible for only 2% of the hydraulic conductance. The "small pores" correspond to the gaps between the endothelial cells and the "large pores" correspond to the venular interendothelial pathways. These ultrasmall pores (2.3 to 15 Å) are permeable only to water (reflection coefficient is unity for all solutes) and were later shown to represent the aquaporin (AQP-1) water channels. AQP-1 was first identified in animal biopsies one year after Rippe proposed its existence [48]. Yang et al. showed that knocking out the aquaporin channels in mice reduced the water transport by 50%, thus proving the importance of the transcellular pores in the three-pore model [49]. The Rippe model can also predict the transport of intermediate solutes as well as large solutes with reasonable accuracy.

Venturoli et al. proposed a series of two porous membranes (Figure 3C)) to model the bi-directional clearances of macromolecules [50]. The first layer is the three-pore membrane by Rippe, identified as the capillary endothelium. This is followed by a second three pore membrane consisting mostly of large pores (95%), transcellular pores (2%), and small pores (3%), which is a lumped representation of extracellular interstitium. This model is able to mathematically explain the build-up of tracer albumin [51] seen in rats, which the one layer three pore model cannot.

Another approach to modeling the peritoneal membrane is the distributed model by Flessner et al. [39] (Figure 3D)). They model the peritoneal tissue space as a tube-and-shell exchanger with a constant void space (blood capillary or the plasma space) and the interstitium. Water movement occurs throughout the tissue while solute convection occurs only across the plasma capillaries. All plasma capillaries are assumed to have the same shape and size, which makes this a single pore model. This model is also complementary to the Venturoli model [50] in that it enables calculation of accumulation and release of certain substances dissolved in dialysis fluid. Because of the additional modeling of the surrounding tissue space, the Flessner model can give insight into the mechanisms ongoing in the peritoneal tissue which could, for example, be useful for modeling transport of drugs being administered intra-peritoneally.

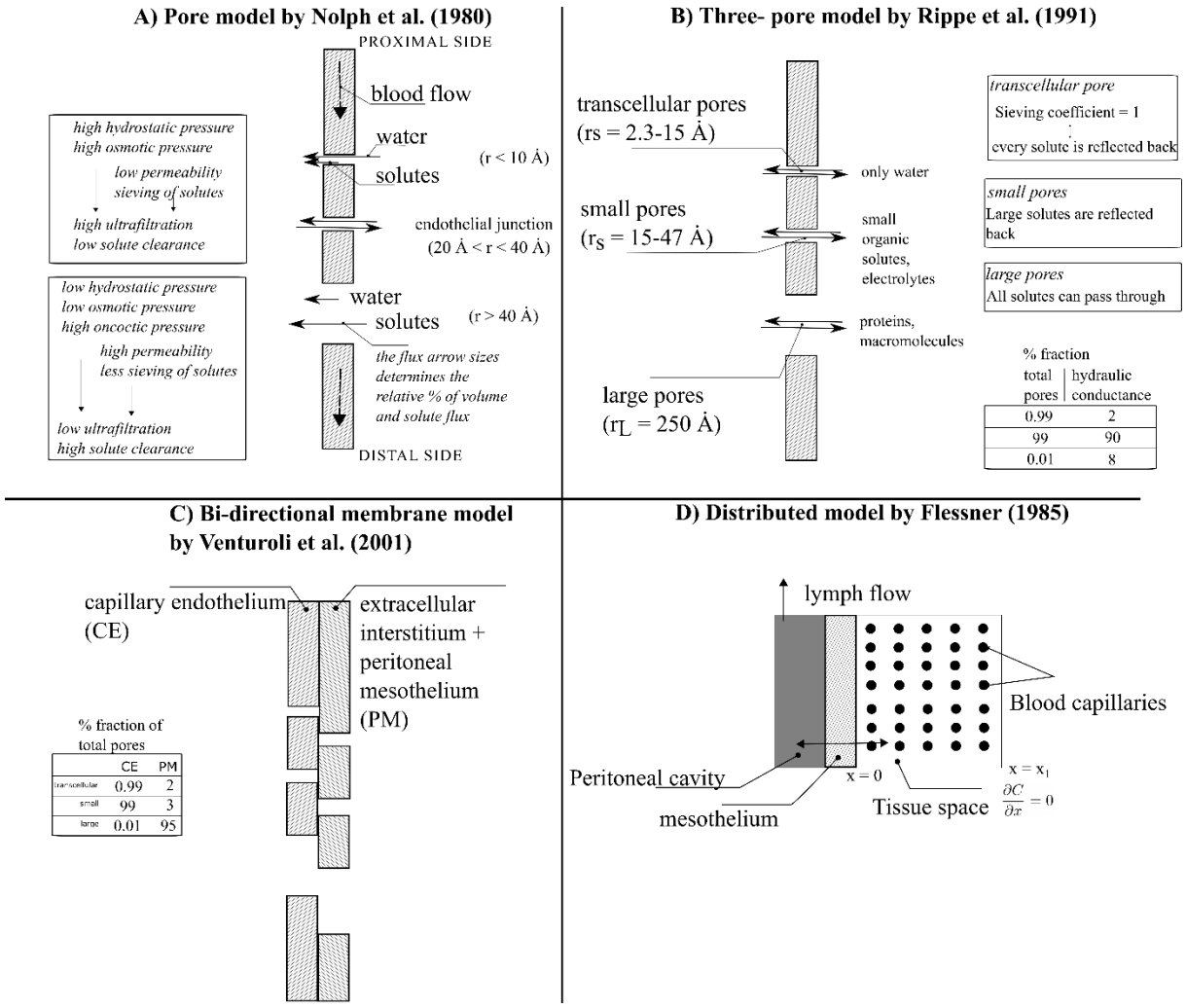

Figure 3. A) Nolph three-pore model (high permeable and low permeable pores), B) Rippe three-pore model (distinction based on size, population and contribution to ultrafiltration), C) Venturoli model (two porous membrane side-by-side), and D) Flessner distributed model (tissue space with uniformly distributed capillaries- essentially a "single pore model" for the capillaries).

3. Volume flow calculations

The osmotic gradient created by a hypertonic dialysis fluid drives the flow of water from the plasma by osmosis, commonly referred to as ultrafiltration [52]. In APD, underestimation or overestimation of the ultrafiltration volume may result in setting a wrong drain volume of the peritoneal cavity. The use of wrong drain settings may cause discomfort to the patient and reduce the efficiency of the dialysis session. As such, it is important to properly calculate all the flows occurring during PD, i.e., the amount of net ultrafiltrate as determined by

- the glucose concentration used in the dialysis fluid and subsequent water flow due to the osmotic gradient
- the flow of dialysate into the peritoneal cavity at a certain flow rate (APD, CFPD) or by gravity (static dwell, CAPD)

- the lymphatic flow of fluid from the intraperitoneal space towards the lymphatic space
- other physical (and patient-specific) attributes such as the condition of the peritoneal membrane, intraperitoneal volume and pressure and the lymphatic system of the patient etc.

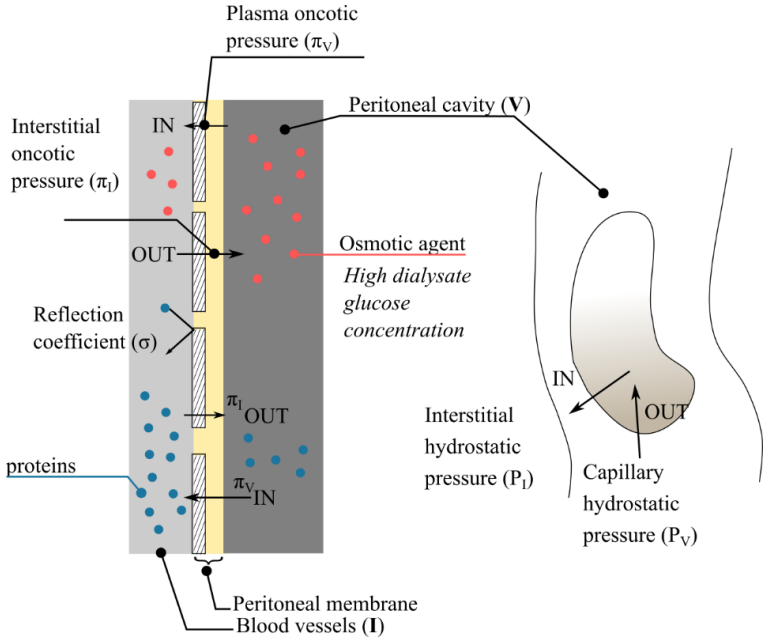

Figure 4. Fluid flow and solute movement across the peritoneal membrane due to hydrostatic pressures and osmotic gradient (see text). A high concentration glucose solution (red dots) is used, which means that the glucose gradient is in a different direction at the beginning of the dwell compared to that of other solutes and proteins (blue dots), which are usually in equilibrium or lower in the dialysate. The striped boxes represent the peritoneal membrane with three types of pores (Section 2.1). I denotes interstitial parameters and V denotes the plasma parameters. IN = from dialysate to blood and OUT = from blood to dialysate.

There have been limited efforts to model volume change in the intraperitoneal cavity. We describe the different ways of estimating peritoneal volume change and the ways to obtain the parameters for the flux equations in further subsections.

To describe the water flow (volume flow), the Starling equation is often used, which is essentially a modified version of Ohms law, $\text{Flow} = \text{Hydraulic conductance} \cdot \Delta\text{Pressure}$. The original Starling equation was written to describe the fluid flow from a capillary to the interstitial space [53]. This equation was later corroborated by Kedem and Katchalsky from a thermodynamics point of view [54]. As fluid builds up in the peritoneal cavity, it exerts an outward interstitial force on the peritoneal membrane (P_I, Figure 4). Due to the fluid moving into the interstitial space, the corresponding fluid pressure rises, and this opposing pressure is the capillary hydrostatic pressure (P_V, Figure 4). The plasma proteins exert a colloid osmotic pressure or oncotic pressure (π_V, Figure 4) to draw water back from the peritoneal cavity to the plasma (opposite to glucose). The osmotic agent in the dialysate exerts an outward osmotic pressure (π_I, Figure 4). To model the above, Eq (4) consists of two inward forces,

i.e., interstitial hydrostatic (P_{I}) and plasma colloid osmotic pressure (π_{V}), and two outward forces, i.e., hydrostatic pressure (P_{V}) and interstitial osmotic pressure (π_{I}) (see Figure 4). Here, we will also take into account that the peritoneal membrane is semi-permeable and will have different reflection coefficients for solutes of different sizes. Note that by inward or outward, we mean into or out of the peritoneal cavity. We refer the reader to the appendix for an overview of all notations.

The volume flow (ml min^{-1}) across the peritoneal membrane is thus modeled as follows:

$$\frac{dV}{dt} = J_v = L_p S[(P_I - P_V) - \sigma(\pi_I - \pi_V)] \tag{4}$$

$$= L_p S\left[\overbrace{\widetilde{\Delta P}}^{hydrostatic\ pressure\ diff} - \sigma \underbrace{\Delta\pi}_{osmotic\ pressure\ diff}\right]$$

The volume in the peritoneal cavity is V, the hydraulic conductance of the peritoneal membrane is given by $L_p S$ (ml $\mathrm{min}^{-1}\mathrm{mmHg}^{-1}$), and the reflection coefficient of the solute is given by σ (dimensionless). I denotes interstitial parameters and V denotes the plasma parameters. We have to make certain modifications to Eq (4) as the fluid is not in full contact with the peritoneal membrane, which means that the whole membrane surface cannot be taken into account for the calculation of the volume flow but rather the peritoneal surface area in contact with the dialysis fluid (af, fraction of the peritoneal surface area in use, dimensionless). This gives us the modified Starling equation (Eq (5)).

$$J_{\mathrm{v}} = L_p S[\Delta P - \sigma \Delta\pi] af \tag{5}$$

In addition to the fractional peritoneal surface area in use, we can divide the volume flow among the various types of pores present in the peritoneal membrane. If we use the classical 3-pore model here, we can divide the net volume flow into flows across the ultrasmall, small, and large pores by multiplying their contribution to the ultrafiltration (α, dimensionless).

$$J_{\mathrm{vC}} = L_p S[\Delta P - \sigma \Delta\pi] \cdot af \cdot \alpha_{\mathrm{C}} \tag{6}$$

$$J_{\mathrm{vS}} = L_p S[\Delta P - \sigma \Delta\pi] \cdot af \cdot \alpha_{\mathrm{S}} \tag{7}$$

$$J_{v\mathrm{L}} = L_p S[\Delta P - \sigma \Delta\pi] \cdot af \cdot \alpha_{\mathrm{L}} \tag{8}$$

where J_{vC}, J_{vS} and J_{vL} are the volume flows across the ultrasmall, small, and large pores, respectively.

The change in volume is then calculated as a total of all the volume flows minus the net lymphatic flow [38],

$$\frac{dV}{dt} = J_{vC} + J_{vS} + J_{vL} - L \tag{9}$$

where L is the lymphatic flow rate (ml min^{-1}) (a sum of all lymphatic flows that drain the peritoneal cavity, i.e., interstitial, diaphragmatic, pelvic and omental [55]), considered to be around 0.15–0.5 ml min^{-1} (0.216–0.72 L/day).

Öberg *et al.* extended Eq (9) for APD [56] and CFPD [38],

$$\frac{dV}{dt} = J_{vC} + J_{vS} + J_{vL} - L + J_{fill} - J_{drain} \tag{10}$$

where J_{fill} and J_{drain} are the fill and drain flow rates during CFPD (ml min^{-1}).

The initial fill volume and drain volume are in general known. The residual volume, V_{r}, may be estimated from the dilution of a solute concentration (e.g., albumin, creatinine, or total protein) measured in the drained effluent, by measuring concentration just after instillation of a known fill volume V_{fill} [57] (Eq (11)):

$$V_r = \frac{V_{fill} * c_0}{(c_{drain} - c_0)} \tag{11}$$

where c_0 is the measured concentration of the solute just after filling the peritoneal cavity (rapid mixing is assumed), and c_{drain} is the concentration of the solute in the drain bag collected in the previous session. Knowing these volumes, the net ultrafiltration volume, UF, can be calculated as,

$$(Net)UF = V_{drain} + V_{r,t2} - V_{fill} - V_{r,t1} \tag{12}$$

where $t1$ is the time of instillment of the dialysis fluid and $t2$ is the time of draining.

Lymphatic flow may or may not be considered depending on the patient and the model. Volume flows are also estimated assuming that the rate of ultrafiltration is known or can be calculated [58].

3.1. How to estimate volume flow parameters?

Few parameters are derived from experimental observations and some are obtained from optimization of models.

3.1.1 Residual Volume, V_r

Residual volume, V_{r}, is a critical factor for accurate assessments of peritoneal membrane parameters such as osmotic conductance to glucose (Section 3.1.4). Clinical conditions such as constipation, catheter position or dysfunction, intraperitoneal adhesions or changes in peritoneal cavity compliance can affect residual volume. The residual volume may be estimated from the dilution of a solute (e.g., albumin, creatinine, urea, total protein, dextran 70 or inulin [59]) after a fresh fill calculated with the concentrations measured in the drained effluent and in the fresh fill just after the instillation of a known fill volume V_{fill} [57] (Eq (13)):

$$V_r = \frac{V_{fill} * c_0}{(c_{drain} - c_0)} \tag{13}$$

where c_0 is the measured concentration of the solute just after filling the peritoneal cavity (rapid mixing is assumed) and c_{drain} is the concentration of the solute in the drained effluent. Urea and

creatinine-based calculations lead to an overestimation of V_r and can be handled with a correction factor [60]. Albumin-based volumes conformed strongly with three-pore model estimates [60].

3.1.2 Difference in hydrostatic pressure, ΔP

The hydrostatic pressure difference between the interstitium and the capillaries in most organs is usually around 10–17 mmHg (13.6–23.1 cm H_2O) [61]. Durand et al. measured the mean intraperitoneal hydrostatic pressure (IPP) to be 9.56 mmHg (13 cm H_2O) [62]. However, in the case of a static PD dwell, the pressure builds up inside the peritoneal cavity due to ultrafiltration so that IPP is a function of time for a patient in a sitting position. Twardowski et al. derived the empirical formula for dependence of IPP as a function of intra-peritoneal volume as follows [63],

$$\Delta P = \Delta P_0 + \frac{V_t - (V_{fill} + V_r)}{490} \tag{14}$$

where ΔP_0 is the baseline hydrostatic pressure (without dialysate), $V_{\text{fill}}, V_{\text{r}}$, and V_t are the initial fill volume, residual volume, and the intraperitoneal volume at time t, respectively. V_{fill} is known (1.0–2.5 l depending on the patient), and the residual volume V_{r} is calculated from eq 13. The peritoneal volume at different times, V_{t}, can, for example, be calculated from the dilution of radioactive ^{125}I serum albumin (RISA) [64,65] during the dwell or from a direct volume recovery technique [66]. 490 comes from the slope of the fitting equation of intra-abdominal pressure versus intra-peritoneal volume, as measured by Twardowski et al. [18].

For continuous flow PD, the hydrostatic pressure changes depend on drain and fill flow rates, and will generally decrease (drain) or increase (fill) in line with intra-peritoneal volume.

3.1.3 Reflection coefficients, σ

Sieving or reflection coefficients for solutes can be determined from experiments [67,68] or from analytical equations such as that of Drake et al. [69]

$$\sigma = \frac{16}{3}\lambda^2 - \frac{20}{3}\lambda^3 + \frac{7}{3}\lambda^4 \tag{15}$$

where λ (dimensionless) is the ratio of the solute radius to the membrane pore radius. The reflection coefficients are calculated separately for different pore sizes and solutes.

Another analytic solution widely used for the three pore model is [70],

$$\sigma = 1 - \frac{\left(1 - \frac{\lambda}{3}\right)(1-\lambda)^2[2 - (1-\lambda)^2]}{\left(1 - \frac{\lambda}{3} + \frac{2}{3}\lambda^2\right)} \tag{16}$$

Theoretically, one can also obtain the (steric) reflection coefficient from the equation by Anderson et al. if one knows the equilibrium concentration of the solute on both sides of the peritoneum, i.e., the blood plasma and the peritoneal cavity [71]

$$\sigma = (1 - \Phi)^2 \tag{17}$$

where Φ is the equilibrium partition coefficient (dimensionless), given by $\Phi = \left(\frac{c_1}{c_2}\right)_{\text{eqlb}}$ and c_1 and c_2 are equilibrium concentrations on both sides of the peritoneal membrane.

3.1.4 Osmotic conductance to glucose

The osmotic conductance to glucose (OCG) of the peritoneal membrane is usually calculated from the double mini-peritoneal equilibration test (dm-PET) described by La Milia et al. [72]. OCG is used to measure the ability of the peritoneal membrane to transport water in response to a crystalloid osmotic gradient. It may hold particular value for the long-term follow-up of PD patients to evaluate the integrity of the peritoneal membrane over time and helps to identify patients at risk for encapsulating peritoneal sclerosis [73]. In the clinic, a 60 min dwell 1.5% (~83 mmol/l) glucose is followed by 60 min 4.25% glucose (~236 mmol/l), and the difference between the drained volume is used to calculate the osmotic conductance to glucose (OCG or $\sigma_g L_p S,\ ml\ min^{-1}\ mmHg^{-1}$). Assuming that the initial volume flow is due to osmosis only, from Eq (5), we get

$$OCG = \frac{\Delta J_v}{\Delta\pi_{4.25} - \Delta\pi_{1.5}} = \frac{\Delta J_v}{RT(c_{4.25} - c_{1.5})} \tag{18}$$

$$OCG \approx \frac{V_{4.25} - V_{1.5}}{100} \tag{19}$$

where R is the gas constant (82 $\text{ml} \cdot \text{atm}\,\text{K}^{-1}\,\text{mol}^{-1}$) and T is the absolute temperature (K). Typical values for OCG are between 0.003–0.004 $ml\ min^{-1}\ mmHg^{-1}$. Knowing the reflection coefficient of glucose from Eqs (15) or (16) or from experiments, L_pS can be calculated to be around 0.08 ml/min per mmHg [7,74–76]. OCG may also be derived from a single dwell, as described by Martus et al. [61]. However, it must be noted that a high residual volume limits the reliability of OCG estimation [73].

3.1.5 Fractional peritoneal surface area in contact with the dialysate, af

Keshaviah *et al.* calculated the empirical relationship between fill volume and peritoneal surface area in contact [77,78],

$$af = \frac{16.18(1 - e^{-0.00077.V})}{13.3187} \tag{20}$$

where V is the intra-peritoneal volume and 0.00077 is an empirical constant in ml^{-1}.

The fractional peritoneal surface area (af, dimensionless) in contact with dialysate can also be obtained from stereological experiments by superimposing a grid over the CT scan of the peritoneum [79,80] or by magnetic resonance imaging [81]. The fractional surface area in contact with dialysate is an important determinant of the mass transfer coefficient of solutes. It can be improved

by increasing the fill volume [82], agitating the dialysate, or adding surfactants [83] but the latter has not been tried in humans. Eq (20) has been shown to be identical to the cube-square law for intraperitoneal volumes up to ~2300 ml [38].

3.1.6 Contribution to hydraulic conductance, α

Fractional hydraulic conductances (α) may be estimated by fitting the experimental results to the model [50,78]. The usual values used in the three-pore model are given in Figure 3.

3.1.7 Ultrafiltration rate, UFR

There have been multiple ways of determining ultrafiltration rate ($\mathrm{ml\,min^{-1}}$) throughout the literature. The average ultrafiltration rate may be estimated from the drain, V_{drain}, and fill volume, V_{fill} during a static dwell [58],

$$UFR = \frac{V_{drain} - V_{fill}}{t} \tag{21}$$

The UF rate can also be theoretically calculated [84,85],

$$UFR = L_p S(\Delta P - \sigma\Delta\pi) - L \tag{22}$$

Lymphatic flow is often considered to be constant throughout the dwell.

The UF rate is sometimes calculated as a function of time from the interpolated intraperitoneal volumes [86–91], as the UFR usually decreases during a static dwell [84,92,93].

$$UFR = \frac{V_{t+\Delta t} - V_t}{\Delta t} + L \tag{23}$$

A simple empirical exponential model was used by Randerson et al. to capture the time dependent UFR [94],

$$UFR = A(1 - e^{-\beta t}) \tag{24}$$

where A is a fitting constant and β is the time constant (a value of 0.0192 $\mathrm{min^{-1}}$ was used).

Total ultrafiltrate volume can also be calculated from the dilution of initial dialysate albumin concentration, as done by Krediet *et al.* [95],

$$(Total)UF = \underbrace{\frac{c_{D,0}}{c_{D,t}}V_0 - V_0}_{net\ transcapillary\ UF} - \left(\underbrace{\frac{c_{D,0}}{c_{D,g}}V_0 - \frac{c_{D,t}}{c_{D,g}}V_t}_{lymphatic\ absorption}\right) \tag{25}$$

where $c_{D,0}$ and $c_{D,t}$ are the dialysate albumin concentrations at time 0 and time t, which is the end of the dwell, $c_{D,g}$ is the geometric mean of the dialysate albumin concentration, $\sqrt{c_{\mathrm{D,0}} * c_{\mathrm{D},t}}$, and V_0 and V_t are the intraperitoneal volumes at time 0 and t.

For CFPD, Öberg et al. theoretically derived the following relation for the UF rate [38],

$$UFR = \frac{\sqrt{(J_{fill} + MTAC_{glu})^2 + 4J_{fill}U_{max}} - (J_{fill} + MTAC_{glu})}{2} \tag{26}$$

where J_{fill} is the fill volume (ml min^{-1}), $MTAC_{\text{glu}}$ is the diffusion capacity (ml min^{-1}), and U_{max} is a function of glucose concentration (ml min^{-1}). The equation slightly overestimates the ultrafiltration.

$$U_{max} = RT \cdot OCG \cdot c_{glu} - 3.1 \tag{27}$$

where RT is the product of gas constant and the temperature in degree Kelvin $(mmHg\ mmol^{-1}L)$, OCG is the osmotic conductance to glucose $(ml\ min^{-1}mmHg^{-1})$, and 3.1 is a constant to account for the lymphatics, opposing forces, and hydrostatic pressure gradient for other solutes in plasma.

Gotch also provided an empirical formula for CAPD using a dextrose solution [96],

$$(Total)UF = (184 + 512\ln(\%D))\ (1 - \exp(-0.02t)) \tag{28}$$

where $\%D$ is the w/w dextrose solution (dimensionless) and t is the time elapsed. For other dialysate solutions, similar curves for total UF *versus* time at different concentrations can be drawn to derive an analytical equation. The equation can then be used to determine the dialysate solution for the desired ultrafiltration.

Depending on the importance of ultrafiltration in the objective of the modeling efforts, one can opt for the simplified UFR values such as Eqs (21) and (23) or for patient specific effects Eqs (24) and (28). Eqs (25) or (26) can provide UFR estimates with sufficient precision but require measuring the concentration of albumin at different time-points, or the estimation of OCG and diffusion capacity of glucose, respectively.

4. Solute flow calculations

Solute flow across a semipermeable peritoneal membrane occurs because of two simultaneous processes. The first is diffusion due to the (electro)chemical gradient between the peritoneal cavity and the blood plasma. Glucose and bicarbonate (and/ or lactate), which are usually present in high concentrations in the dialysate, move to the plasma. Other solutes such as potassium, phosphate, and toxins move from the plasma to the peritoneal cavity. The second is "convection" due to the water flow ("ultrafiltration") that drags solutes across the membrane (from the plasma to the peritoneal cavity). There have been many ways of describing solute flow in the literature since small solute clearance was the main priority of many early PD models. In the following sections, we discuss how the solute flows can be calculated depending on the complexity required. In subsections, we also discuss how to obtain parameters for solute flow equations.

The Patlak equation captures such a two-part transport of solutes across the thick inhomogeneous peritoneal membrane (see Eq (29), Figure 5) [97]. The Patlak equation is essentially an extension of the second equation proposed by Kedem and Katchalsky's thermodynamics-driven volume and solute flux across a thin semi-permeable membrane [54]. First, there is a term that models the diffusive flux across the membrane due to the concentration gradient, given by Fick's first law. The second part is

the convective transfer arising from ultrafiltration.

$$J_s = -DA\frac{dC}{dx} + J_v(1-\sigma)C \tag{29}$$

where D is the diffusion coefficient ($m^2 min^{-1}$), and A is the effective surface area available for diffusion (m^2), C is the intramembrane concentration ($mol\ ml^{-1}$), and J_v is the volume flow ($ml\ min^{-1}$).

Rearranging and integrating the ordinary differential Eq (29) gives

$$J_s = J_v(1-\sigma)\frac{c_p - c_D e^{-Pe}}{1-e^{-Pe}} \tag{30}$$

$$Pe = \frac{J_v(1-\sigma)}{MTAC} \tag{31}$$

where c_p and c_D are the plasma and dialysate solute concentration, respectively, Pe is the Péclet number, which is a ratio of diffusional and convectional mass transfer (dimensionless), $MTAC$ is the diffusion capacity ("mass transfer area coefficient") ($ml\ min^{-1}$), σ is the reflection coefficient (dimensionless), and J_v is the volume flow ($ml\ min^{-1}$). For details of the derivation, refer to [74].

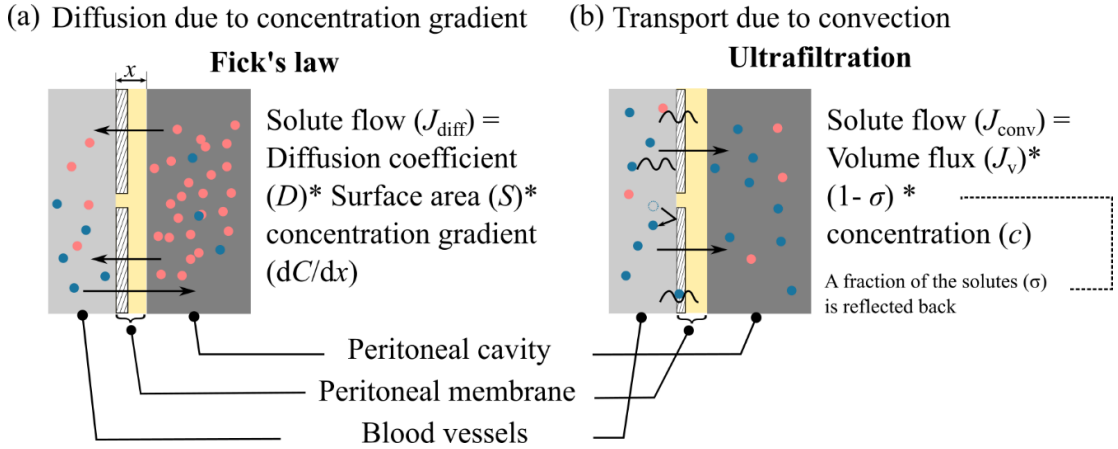

Figure 5. Schematic depiction of the solute flow due to diffusion and convection over the peritoneal membrane.

There are other representations of diffusion and convection in various models. Pure diffusion models are sometimes used to define solute transport such as those by Leypoldt et al. and Villarroel et al. [42,98,99].

$$V\frac{dc_D}{dt} = MTAC\ (c_p - c_D) \tag{32}$$

where V is the peritoneal dialysate volume.

Babb et al. used the following equation to represent the solute flux [58,84] (Eq (33)),

$$V\frac{dc_D}{dt} = MTAC\left(c_{p_0} - c_D\right) + SiCo \cdot \boldsymbol{c} \cdot UFR \tag{33}$$

where $SiCo$ is the sieving or transmittance coefficient or membrane selectivity of the particular solute and UFR is the ultrafiltration rate ($\mathrm{ml\,min^{-1}}$, for calculation of parameter, see Section 3.1.7). Different interpretations of $\boldsymbol{c}$ (mol ml^{-1}) are reported in the literature:

$\boldsymbol{c} = c_p$ *when* UF *is considered from only one direction [58,100] or* UF *is large [84]*

$\boldsymbol{c} = (1-f)c_p + fc_D$ *when* $\boldsymbol{c}$ *is considered as the intramembrane solute concentration [40,85,94]*

$\boldsymbol{c} = \frac{c_p + c_D}{2}$ *when* UF *is low [84]*

here, f is a function of the Péclet number, which is a ratio of convection to diffusion, given by

$$f = \frac{1}{Pe} - \frac{1}{e^{Pe} - 1} \tag{34}$$

Graff and Fugleberg et al. compared six models of the peritoneal solute transport of urea, creatinine, glucose, potassium, and phosphate [86–91], using Eq (35)

$$V\frac{dc_\mathrm{D}}{dt} = \left(\underbrace{MTAC\left(fct \cdot c_\mathrm{p} - c_\mathrm{D}\right)}_{diffusive} + \underbrace{SiCo \cdot UF \cdot \boldsymbol{c}}_{Non-lymphatic} - \underbrace{L \cdot C^*}_{lymphatic} \right) \tag{35}$$

where fct is the equilibrium ratio for solute concentration in dialysate and plasma concentration ($\frac{C_\mathrm{D}}{C_\mathrm{p}}$), $SiCo$ is the sieving coefficient, $\boldsymbol{c}$ is the intramembrane solute concentration to account for the non-lymphatic convective transfer across the peritoneal membrane, and C^* is the concentration in the lymph vessels, which depends on the direction of the lymphatic flow ($C^* = c_\mathrm{D}$ if flow is from peritoneal cavity to lymph (vessels) or else $C^* = c_\mathrm{p}$). They found that glucose transport is purely diffusive while lymphatic flow was important in urea and creatinine transport. Non-lymphatic convective transport is important for urea, creatinine, potassium, phosphate, and sodium with a sieving coefficient close to 1 (all molecules passing through). Their models showcase that one general model cannot be applied across all body solutes but differs depending on the size, concentration, and diffusivity of solutes.

The lymphatic flow is denoted by L. Other studies that have included lymphatics flow are Waniewski et al. [101], who show that MTAC values are underestimated for total protein if lymphatic flow is neglected (Eq (36)).

$$V\frac{dc_D}{dt} = \left(MTAC\left(c_p - c_D\right) + (UFR + L)\left[(1-f)c_p + fc_D\right] - Lc_D\right) \tag{36}$$

The fitting constant f is usually to be fitted for all solutes separately, but an assumption of 0.5

works for most small solutes excluding sodium [92].

So far, we have mainly discussed compartmental ODE models. Some efforts have included PDE descriptions of the PD process. For example, multi-compartment models such as those by Flessner et al. [39,102], consider the mass transfer from the capillaries into the surrounding peritoneal tissue and lymphatics to be contributors for solute flux in the peritoneal cavity.

$$\frac{dVc_D}{dt} = \left(\underbrace{af \cdot S \cdot \frac{D_t}{\tau} \cdot \frac{\partial c_t}{\partial x}\Big|_{x=0}}_{diffusion} - \underbrace{rJ_v{}'\,(af \cdot S) c_t|_{x=0}}_{convection} \right) - Lc_p \tag{37}$$

where af is the fractional peritoneal surface area in contact with the fluid (Section 3.1.5), c_t is the concentration of the solute in the surrounding tissue, S is the surface area of the peritoneal membrane (m^2) and, D_t is the diffusion coefficient in the tissue ($m^2 min^{-1}$), τ is the tortuosity (dimensionless), r is the retardation factor (dimensionless), L is the lymphatic flow rate (ml min^{-1}), c_p Is the blood plasma concentration (mol ml^{-1}), and $J_v{}'$ is the local volume flux at distance x into the tissue (ml $m^{-2} min^{-1}$).

$$J_{\mathrm{v}}'|_x = (J_{\mathrm{v}} a x_t - J_{\mathrm{v}} a x)/(af \cdot S) \tag{38}$$

where a is the capillary surface area per unit tissue (m^{-1}) and x_t is the thickness of the tissue (m). The distributed model is used to study fluid absorption and swelling of peritoneal tissue during peritoneal dwell [102,103]. Spatial models can also be utilized to monitor the penetration of medications, such as chemotherapeutics, administered into the peritoneal cavity. Other spatial models can be found in [104,105].

Gotch added the drain flow rate ($= J_{fill} + UFR$) to derive the solute flux into the peritoneal cavity for single pass CFPD as [96] (Eq (39)),

$$V \frac{\mathrm{d}c_D}{\mathrm{d}t} = \left(MTAC\left(c_{\mathrm{p}} - c_{\mathrm{D}}\right) + UF \cdot SiCo \cdot \left(0.67 c_{\mathrm{p}} + 0.33 c_{\mathrm{D}}\right) - \left(J_{\mathrm{fill}} + UFR\right) c_{\mathrm{D}} \right) \tag{39}$$

Öberg et al. used the three-pore model for both volume and solute flux for CFPD [38]. Volume fluxes are represented in Eqs (6)–(8). Using the volume flux and Patlak equation (Eq (30)), they calculated the solute fluxes as Eq (40),

$$V \frac{\mathrm{d}c_{\mathrm{D}}}{\mathrm{d}t} = J_{\mathrm{sS}} + J_{\mathrm{sL}} - c_D (J_{\mathrm{vC}} + J_{\mathrm{vS}} + J_{\mathrm{vL}} + J_{\mathrm{fill}}) + c_{\mathrm{D0}} J_{\mathrm{fill}} \tag{40}$$

where J_{sS} and J_{sL} are the solute fluxes over the small and large pores (solute flux over the ultrasmall pores is non-existent).

Icodextrin is a mixture of different dextrin molecule fractions (molecular weight ranging from 12–20 kDa). Briefly, for icodextrin modeling, an additional term is added that refers to the hydrolysis of the higher molecular weight icodextrin fraction, caused by the enzyme α-amylase.

$$V\frac{\mathrm{d}c_{\mathrm{D}}}{\mathrm{d}t} = J_{\mathrm{sS}} + J_{\mathrm{sL}} + \sum_{j=1,2,\ldots,7} r_i^j V c_{D,amylase} \cdot c_{D,Ico_j} \tag{41}$$

where r_i^j is the appearance rate of icodextrin fraction i due to hydrolysis of fraction j ($ml\,U^{-1}min^{-1}$), $c_{D,amylase}$ is the amount of amylase (U), and c_{D,Ico_j} is the fraction j of icodextrin [6,106]. 1 unit (U) is the amount of enzyme that catalyzes the reaction of 1 μmol of substrate per minute.

From Eq (30),

$$J_{sS} = J_{vS}(1-\sigma)\frac{c_p - c_D e^{-Pe,S}}{1 - e^{-Pe,S}} \tag{42}$$

$$J_{sL} = J_{vL}(1-\sigma)\frac{c_p - c_D e^{-Pe,L}}{1 - e^{-Pe,L}} \tag{43}$$

where Pe is calculated from Eq (31).

J_{vC}, J_{vS}, and J_{vL} are the volume fluxes over the three types of pores, J_{fill} is the fill flow rate and c_{D0} is the solute concentration in the fresh dialysate.

4.1 How to calculate the solute flow parameters

After calculating the volume flow, one can use it to calculate the solute flux. Standard peritoneal permeability analysis (SPA) is a standardized tool used to assess the membrane transport properties of a specific patient. These assessments are then used to determine the PD prescription for the specific patient [107]. For a SPA test, a static dwell is used with regular dialysate sampling and blood sampling [108].

4.1.1 Diffusion Coefficient, D

The diffusion coefficient, D ($\mathrm{m^2 s^{-1}}$) can be calculated for charged and uncharged particles through liquid flow at low flow rates,

$$D = \frac{\mu \mathrm{k_B} T}{q} \tag{44}$$

$$D = \frac{\mathrm{k_B} T}{6\pi\eta r_{\mathrm{s}}} \tag{45}$$

where μ is the electric mobility of the solute $\left(\frac{\mathrm{m^2}}{\mathrm{Vs}}\right)$, k_B is the Boltzmann constant (Joule, J per

Kelvin), T is the temperature (K), q is the charge of the solute (Coulomb), η is the dynamic viscosity $(\mathrm{Pa}\cdot\mathrm{s})$, and r_s is the solute radius (m). Equation (44) is for charged solutes and Eq (45) is for uncharged solutes.

4.1.2 Mass transfer area coefficients, $MTAC$

The capacity for diffusion MTAC ($\mathrm{ml\,min^{-1}}$) is the maximal diffusive clearance and can be calculated from

$$MTAC = D\frac{A_0}{\Delta x}\frac{A}{A_0} \tag{46}$$

where $A_0/\Delta x$ is the unrestricted surface area to diffusion length ratio (in cm). Typically, a patient with an average peritoneal solute transfer rate has an $A_0/\Delta x$ of 25,000 cm, whereas a value < 16,000 cm or > 40,000 cm may indicate slow- and fast peritoneal transport, respectively. The factor A/A_0 represents the diffusive hindrance factor and is usually estimated using the equation by Mason, Wendt, and Bresler [70], as follows

$$\frac{A}{A_0} = \frac{(1-\lambda)^{9/2}}{1 - 0.3956\lambda + 1.0616\lambda^2} \tag{47}$$

where λ is the solute to membrane pore radius ratio. MTAC may also be estimated from experimental data [92,100,109]

$$MTAC = \frac{V_t}{t}\ln\frac{V_0^{1-f}(c_p - c_{D,0})}{V_t^{1-f}(c_p - c_{D,t})} \tag{48}$$

where V_t and V_0 is the intraperitoneal volume at time t and 0, f is from Eq (34) and $c_{D,0}$ and $c_{D,t}$ is the dialysate solute concentration at time 0 and t, respectively, and c_p is the plasma solute concentration.

Keshaviah et al. compared different functions for MTAC and found that the parabolic and negative exponential functions for urea, creatinine, and glucose best fit the dialysate volume profile [77],

$$MTAC = a_1 + a_2V + a_3V^2 \tag{49}$$

$$MTAC = a_1[1.0 - \exp(a_2V)] \tag{50}$$

where a_1, a_2, a_3 are fitting constants that are different for each of the three solutes.

4.1.3 Sieving coefficients, $SiCo$

The sieving coefficient, $SiCo$ (dimensionless), is usually fitted in a model [58,86–91], microscopy study [110] or calculated from experimental observations such as the formula derived by Chen et al. [67],

$$SiCo = \frac{1}{c_{\mathrm{p}}}\left(\frac{c_{\mathrm{D},t}\,V_t + c_{\mathrm{D},g}\,Cl_{\mathrm{albumin}} - c_{\mathrm{D},0}V_0}{V_{\mathrm{UF}}}\right) \tag{51}$$

where V_t and V_0 is the intraperitoneal volume at time t and 0, respectively, $c_{\mathrm{D},0}$ and $c_{\mathrm{D},t}$ are the dialysate solute concentration at time 0 and t, respectively, and c_{p} is the plasma solute concentration, V_{UF} is the net ultrafiltration volume, and Cl_{albumin} is the clearance of albumin.

Rippe et al. also calculated the sieving coefficient incorporating hematocrit [111],

$$SiCo = 1 - \left(\frac{c_t}{c^*}\left\{1 - \left[\frac{(1-H_0)(1-c_0/c_t)}{1-H_0/H_t}\right]\right\}\right) \tag{52}$$

where H_0, H_t are the initial and final hematocrit and c_0, c_t, and c^* are the initial, final and average plasma proteins concentrations.

It can also be simply calculated from the reflection coefficients calculated in Section 3.1.3,

$$SiCo = 1 - \sigma \tag{53}$$

5. Summary of models for peritoneal dialysis

In this section, we provide a comprehensive look at the different models of PD that have been developed throughout the years (1966–2019) (Figure 6). We looked for publications that mentioned "kinetic modeling", "mathematical model", "computational model" with "peritoneal dialysis". In total, we found 26 distinct models of PD. We have mentioned what kind of compartments were considered along with what were the main aim/hypotheses of the modeling effort. Modeling was used as a tool to establish the efficiency of a PD model (5 out of 26) [38,41,78,94,112] while four models were designed to understand the fundamentals of solute and volume transport [42,58,98,113]. We have also characterized the types of transport processes were included in the volume and solute transport equations of the model. Three of the 26 models were purely diffusive [41,42,112] while other models (23 out of 26) included convection and diffusion into the surrounding tissue [83,114,115]. Some models were generalized for any type of solute [38,84,115] while some were prepared for specific solutes only [86–91,99]. Different PD modalities can be found in [7,38,51,78,93,116], and models for glucose-sparring solutions are in [6,106,117]. Table 1 shows a consecutive overview of 26 PD models that have been published, and figure 6 shows the evolution of PD models. Depending on the solute(s) or drug and which part of the PD process one is interested in, one can choose any of these models.

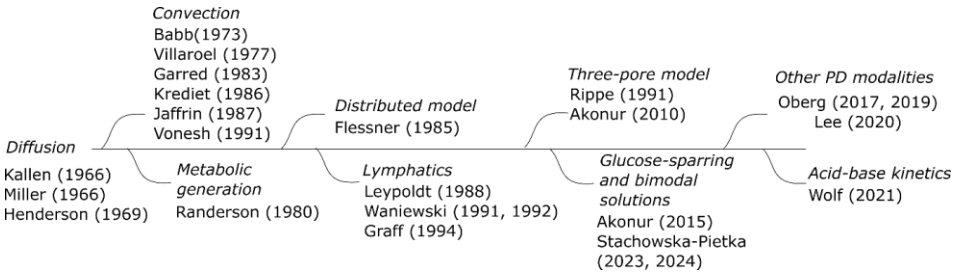

Figure 6. Evolution of PD models starting from the 1960s.

Table 1. Overview of various PD models with different interpretations of volume and solute flux, types of compartments, and PD mode. Some models were developed specifically for a particular type of solute while others can be generalized to other solutes.

Model	Purpose	Type of PD	Method	Volume flux	Solute flux	Solute included	Compartment	Model developed	Ref.
Kallen (1966)	To determine PD efficacy in different body sizes by modeling	Static dwell	Modeling	Osmotic gradient	Diffusion	Urea	Body, Peritoneal cavity	Nomogram	[41]
Miller et al. (1966)	To determine the most efficient mode of APD through clinical studies	Intermittent, Intermittent Recirculating, Continuous, Continuous recirculating, Rapid intermittent, Continuous compound dialysis	Modeling + Clinical (n = 14)	-	Diffusion	Urea, Creatinine, Uric acid	Body, Peritoneal cavity	Algebraic	[112]
Henderson et al. (1969)	To make a mathematical model of peritoneal solute transport by diffusion	Static dwell	Modeling + Clinical (n = 6)	-	Diffusion	Inulin, Urea	Blood, Peritoneal cavity	ODE	[42]

Babb et al. (1973)	To develop a bi-directional mass transfer model for solutes	Static dwell	Modeling + Clinical (n = 3)	Ultra-filtration (constant)	Diffusion, Convection	Urea, Creatinine, Uric acid, Sucrose, Vitamin B12, Inulin	Capillary blood, Peritoneal cavity	ODE	[58]
Villarroel et al. (1977)	To characterize solute clearances for different types of PD with modeling	Intermittent PD, CFPD	Modeling	Outgoing flow rate	Diffusion (intermittent), Diffusion + convection (continuous)	Urea	Blood, Peritoneal cavity	Algebraic	[99]
Randerson et al. (1980)	To determine whether a two-pool or three-pool model represents solute transfer in CAPD	CAPD	Modeling + Clinical (n = 15)	No flux	Diffusion, Convection, Metabolic generation, Residual renal clearance	Urea, Creatinine, Vitamin B12	Body + Peritoneal cavity (Urea, Creatinine), Extracellular compartment + intracellular compartment + Peritoneal cavity (B12)	ODE	[94]
Garred et al. (1983)	To develop a model for mass transfer in CAPD	CAPD	Modeling	Ultrafiltration (constant)	Diffusion, Convection	Urea, Creatinine, Vitamin B12	Blood, Peritoneal cavity	ODE	[100]

Flessner et al. (1985)	To develop a model of peritoneal transport that includes diffusion and convection into the surrounding tissue	Static dwell	Modeling	Osmotic gradient, Ultrafiltration, Lymphatics	Diffusion, Convection	Sucrose	Peritoneal cavity, Peritoneal tissue, Distribution volume, Body exchange compartment	PDE	[39]
Krediet et al. (1986)	To determine MTAC for different solutes by a first order kinetic model of solute mass transfer	CAPD	Modeling + Clinical (n = 11)	Ultrafiltration (constant)	Diffusion, Convection	Urea, Lactate, Creatinine, Glucose, Kanamycin, Inulin	Blood, Peritoneal cavity	ODE	[109]
Jaffrin et al. (1987)	To determine the peritoneal solute concentration and volume variation in CAPD using a one-pool model varying dwell time and glucose concentration	CAPD	Modeling	Osmotic gradient	Diffusion, Convection	Solute independent	Blood, Peritoneal cavity	ODE	[84]

Mactier et al. (1988)	To determine the impact of peritoneal cavity lymphatic absorption on ultrafiltration and solute clearances	CAPD	Modeling + Clinical (n = 10)	Ultrafiltration, Lymphatics	-	Creatinine, Glucose	-	Algebraic	[113]
Leypoldt et al. (1988)	To distinguish between indicator dilution volume and true dialysate volume	Static dwell	Modeling + experiment (rabbit, n = 9)	-	Diffusion, Lymphatics	Creatinine	Blood, Lymphatics, Peritoneal tissue	ODE	[98]
Vonesh et al. (1991)	To use modeling as a tool to predict fluid and mass removal and guide selection of PD type for patients	CCPD, Tidal PD	Modeling + Clinical (n = 5, different PD types)	Osmotic gradient, Lymphatics	Diffusion, Convection	Urea, Creatinine, Glucose, $\beta 2$ micro-globulin	Body, Peritoneal cavity	ODE	[85]
Waniewski et al. (1991)	To simplify Garred model [100] for small solute transport	Static dwell	Modeling + clinical studies (n = 21)	Ultrafiltration (constant)	Diffusion, Convection	Urea, Creatinine, Glucose, Potassium, Sodium, Protein	Blood, Peritoneal cavity	Algebraic	[92]

Rippe (1991)	To develop a new model for CAPD assuming the peritoneal membrane is mainly composed of three types of pores (TPM)	CAPD	Modeling	Ultrafiltration, Lymphatics	Diffusion, Convection	Glucose, Urea, Sodium, Albumin, Phosphate, $\beta 2$ microglobulin	Body, Cavity	Peritoneal	ODE	[7]
Waniewski et al. (1992)	To develop simple membrane models for diffusive and convective solute transport	Static dwell	Modeling + Clinical (n = 20)	Ultrafiltration	Diffusion, Convection	Urea, Creatinine, Sodium, Potassium, Glucose, Total protein	Body, cavity	Peritoneal	ODE	[118]
Graff and Fugleberg (1994)	To determine the best solute transport mechanism for different solutes	Static dwell	Modeling + Clinical (n = 21 to 26)	Ultrafiltration, Lymphatics	Diffusion, Convection (non-lymphatic and lymphatic)	Urea, Glucose, Phosphate, Creatinine, Potassium, Sodium	Body, Cavity	Peritoneal	ODE	[86–91]
Gotch (2002)	To develop a kinetic model of CFPD	Single pass CFPD	Modeling	Ultrafiltration	Diffusion, Convection	Urea	Body, cavity, (External Dialyser)	Peritoneal	ODE, Empirical	[96]

Akonur et al. (2010)	To use TPM for optimization of drain phase in static dwell	Static dwell	Modeling	Ultrafiltration, Lymphatics, Biphasic equation for drain	Diffusion, Convection, Lymphatics	Urea	Body, Cavity	Peritoneal	ODE	[119]
Akonur et al. (2015)	To modify TPM to include α-amylase activity in icodextrin kinetics	Static dwell	Modeling	Ultrafiltration, Lymphatics	Diffusion, Convection, Lymphatics, First order degradation of higher weight fractions of icodextrin	Icodextrin	Body, Cavity	Peritoneal	ODE	[106]
Oberg et al. (2017)	To extend classic TPM to include the fill and drain phases of dwell.	APD	Modeling	Ultrafiltration, Lymphatics	Diffusion, Convection, Lymphatics	Glucose, Urea, Sodium, Phosphate, $\beta 2$ microglobulin, Creatinine, Total protein	Body, Cavity	Peritoneal	ODE	[56]

Oberg et al. (2019)	To extend TPM for CFPD and determine the ultrafiltration rate	CFPD	Modeling	Ultrafiltration, Lymphatics	Diffusion, Convection, Lymphatics	Glucose, Urea, Sodium, Phosphate, $\beta 2$ microglobulin, Creatinine, Total protein	Body, Cavity	Peritoneal	ODE	[38]
Lee et al. (2020)	To model steady (glucose) concentration PD (SCPD) with continuous glucose infusion	SCPD	Modeling	Ultrafiltration, Lymphatics	Diffusion, Convection, Lymphatics, Infusion of glucose	Glucose, Urea, Sodium, Creatinine, Total Protein	Body, Cavity	Peritoneal	ODE	[120]
Wolf et al. (2021)	To extend TPM to determine acid-base kinetics during PD	Static dwell	Modeling	Ultrafiltration, Lymphatics	Diffusion, Convection, Lymphatics, CO_2 conversion to bicarbonate	Glucose, Urea, Sodium, Phosphate, Total protein, Lactate, Bicarbonate, Calcium, Magnesium	Body, Cavity	Peritoneal	ODE	[121]

Stachowska-Pietka et al. (2023)	To modify TPM to include α-amylase activity in icodextrin kinetics	Static dwell	Modeling + Clinical (n = 11)	Ultrafiltration, Lymphatics	Diffusion, Convection, Lymphatics, First order kinetics of icodextrin hydrolysis including α-amylase concentration	Glucose, Creatinine, Icodextrin	Body, Peritoneal Cavity	ODE	[117]
Hartinger et al. (2023)	To make a population pharmacokinetic model of vancomycin	Static dwell	Modeling + Clinical (n = 41)	-	First order clearance	Vancomycin	Peritoneal cavity, one and two-compartment models for rest of the body	PK	[122]

ODE, Ordinary differential equations (Assume that the compartment is homogeneously mixed); PDE, Partial differential equations (distribution within the compartment is important); MTAC, Mass transfer are area coefficient; TPM, Three-pore model; PK, Pharmacokinetic model (series of ODE to describe the rates of drug absorption, distribution, metabolism and elimination to predict drug concentration changes over time); PD, Peritoneal Dialysis; APD, Automated PD; CFPD, Continuous flow PD; CAPD, Continuous Ambulatory PD; CCPD, Continuous cycling PD.

6. Test case for developing a mathematical model of PD

Many PD-related questions can be answered with mathematical modeling, for example:

- What is the optimal glucose concentration for PD, balancing ultrafiltration (volume and efficiency) versus adverse effects (e.g., increased peritonitis risk)?
- What is the influence of two catheters *vs* one single lumen catheter on solute clearance in continuous flow *vs* tidal PD?
- How does the intraperitoneal dialysate volume affect solute clearance in CAPD or CFPD?
- Which flow rates are ideal in CFPD?
- What is the clearance of a particular solute/drug for a particular PD modality (CAPD, APD, or CFPD)?
- How does tidal PD with partial drainage of the solution, leaving a residual volume in the peritoneal cavity, affect solute clearance as compared to complete drainage?

In Table 2, we demonstrate how we can create and implement our mathematical model if we know which research question we want to answer, what experimental data or literature data we possess, and what kind of math is necessary for the model. With the realized model, we can then play with the parameters to determine an optimal treatment scenario for the patient, as we can analyze both the short-term and long-term effects of a session.

Table 2. A stepwise approach to design a mathematical model from scratch. An example scenario explains how, with the objective and preliminary data specified, one can further build an existing model to answer a particular PD-related question. 'Drug' in this example can be replaced with any endogeneous solute that is removed by PD.

		Steps to creating a mathematical model	***Example scenario***
1		Clearly specify the problem	What is the clearance of drug X is given to the patient via PD? What is the influence of drug X on solute clearance?
2		Which data are available?	The concentration of solutes (c_D) and drug (c_{drug})in the fluid, device flow rates (J_{fill}, J_{drain}), distribution volume and intra-peritoneal volume, diffusion capacities of the solutes and drug ($MTAC$). $MTAC$ values can be obtained from studies like [123], where they analyze the transport of model compounds according to weight, acidity, partition coefficient (Φ , see Section 3.1.3). Note that an increase in MTAC should be taken into account for CFPD (several-fold increase may occur)
3	INPUT	Are lymphatics involved in removal of this drug?	Depending on the answer, one can put the lymphatic flow rate, L = 0 for the ones that

			do not have lymphatics involved at all. Certain drugs might inhibit solute transport to blood but encourage lymphatic transport [124,125].
4		Is the drug removed primarily by diffusion (as is glucose) or also via convection?	There are many studies for drug clearance by peritoneal membrane, especially antibiotics and chemotherapy drugs [126,127]. Dedrick et al. designed a pharmacokinetic model of drug clearance by the peritoneal membrane to select the one better suited for a clinical trial [128]. Having an idea of the removal kinetics would help to choose between a diffusion only model [41,112] or convection + diffusion model [38,96].
5		Is the solute clearance inhibited by the drug X?	Studies show that drugs like furosemide or ACE inhibitors might inhibit solute transport across the peritoneal membrane [129,130]. This can be modeled by a reduced $MTAC$ for the solute in question.
6		Does the drug penetrate the surrounding tissue?	Dedrick *et al.* have shown in their model that for slowly reacting drugs there can be surface penetration up to $(D/k)^{0.5}$, where D is the diffusivity of the drug and k is the rate constrant of drug removal from tissue [131]. If significant, it might be necessary to use the Flessner model [115].
7		Is it a static dwell or continuous flow model?	Static dwell model such as [89,92,98] or continuous flow model like [78,96,109] could be chosen.
8		Are time series data of the dialysate solute concentration available?	If yes, the model that is chosen in the steps 3–7 could be fitted to obtain the correct $MTAC$ value or other previously assumed parameters. If no, with the PD effluent, one can estimate the average $MTAC$ during a particular session. Note that, in both cases, average $MTAC$ is most often estimated as the parameter that decreases during the dwell time [77].
9	OUTPUT	Can clearance be calculated?	With a precise parameter set, clearance of drug X and other solutes can be calculated in any time range for a specific patient.

7. Discussion

In this review, we give an overview of the physical principles that govern peritoneal dialysis and summarize the essential (differential) equations for volume and solute flux that are required to model peritoneal dialysis. These models are sometimes based on simple principles and parameters are lumped together to study a compartmentalized version of the body [41,58,86–91], while other models are very complex and require many parameters to capture the physical processes in depth [38,102,115]. In this review, we chose to focus more on the time dimensional models, and thus a spatial model discussion is out of scope. However, spatial models can be found in [39,83,103–105,114,115]. We have also not included other glucose-sparring solutions that have been modelled, and valuable information on this can be found in [6,106,117]. We also list different ways the in which various simulation parameters are obtained. Most often, parameters are derived directly from patient data (effective peritoneal surface area, dialysate clearance, etc.), some of the parameters are derived from analytical formulae (reflection coefficient, hydrostatic, and osmotic pressure difference), others are derived from the model itself (ultrafiltration, pore contribution to ultrafiltration, and fractional hydraulic conductance), and some parameters may be fitted to obtain the best (patient-specific) interpretation of the dialysate and plasma solute concentration. Each model can be modified to fit the required patient data and get outputs such as ultrafiltration rate, mass transfer area coefficients, and residual volumes. From Eqs (15) and (16), we do not see a significant difference in the estimation of sieving coefficients (Supplementary Figure 1). This underlines the fact that multiple studies have been done to converge on the most optimal values of reflection coefficients. However, we must note that reflection coefficients and thus, sieving coefficients may differ with prolonged exposure of the membrane to glucose and glucose-degradation products. This highlights a critical gap in the literature, necessitating further investigation to refine these parameters for enhanced model accuracy.

The human body is a complex system, which makes it difficult to model. Modeling its various parts should eventually lead us to understand the whole. Over the years, PD models have generally included more and more transport processes. The first PD models were purely diffusive which is representative of small molecular transport such as that of urea and creatinine [41,42,112]. As the importance of middle-sized molecules became appreciated, convection was added to the models, as this is an important route to eliminate these compounds [58,99]. Lymphatic absorption [38,96] and peritoneal tissue surface area [115] have since been added to the models. As per the new ISPD guidelines, ultrafiltration is a crucial parameter to determine the efficacy of a PD treatment [132]. Thus, we see that recent models are also trying to model time-dependent ultrafiltration in patients [38]. This requires rigorous evaluations and comparisons of ultrafiltration rates. In Section 3.1.7, we discuss multiple ways to obtain ultrafiltration rate and which efforts can be made to make the best estimate.

With an increase in computational power and physical understanding, the model complexity can be increased to create a better picture of the underlying mechanisms in the patient's peritoneal cavity. Herein lies a caveat. The increased complexity makes the model space hyper-parameterized. Thus, finding efficient parameter combinations that satisfy physiological relations is difficult to achieve without multiple assumptions. This can be achieved by fitting parameters to clinical data (for example, in [133], Stachowska-Pietka et al. fitted 16 parameters while assuming 9 parameters to be fixed) and calibrating the model in a different scenario (they showed that the predictions of interstitial concentration of mannitol in rat abdominal wall were in agreement with experiments [133]). Future models can be improved to include metabolism of glucose in the peritoneum, and vascular

inflammation [134] and how these affect the peritoneal membrane, positioning of catheters in patients and cellular contributions to the solute clearances (for example for glucose [135]). Future PD models can also be made spatial (using for example partial differential equations) to understand the spatial influence of flow and the solute gradient. How does the continuous flow change the boundary layer of the peritoneal membrane? What happens to the residual volume? What fraction of recirculation occurs just at the tip of the catheter? Can patient-reported outcome measures be linked to PD (efficacy) parameters? Partial differential equation modeling (used for space localisation) of the peritoneal cavity may help us answer these questions. Agent based modeling (ABM) can also be helpful in this aspect. ABM models take into account different agents (e.g., patient characteristics, residual kidney function, smoking, dietary habits, transport status, sex, weight, and osmotic agent, etc.) to assess the problem and make decisions based on a complex behavioral pattern. ABM models have already been used to determine the optimum treatment pathway for HD patients based on patients', nephrologists', and surgeons' attributes [136]. From recent developments in PD, we definitely see that patient membrane characteristics and preferences play a huge role in managing the patient. Efforts have already been made in the past to suggest the best mode of PD treatment for different patient characteristics [38,85,99,112,137] but more work needs to be done on personalizing a single PD mode based on the sex, age, weight, peritoneal characteristics, and residual kidney function of the patient. Nevertheless, there are many aspects that a virtual PD system cannot cover, such as catheter dysfunction and nonadherence to medication.

We can picture the growth of mathematical modeling of PD in two complementary directions: Fundamental understanding and personalization. More technical components can be introduced to the existing models, and parameters can be analyzed to facilitate a faster understanding of the new devices and optimize them before market entry. One aspect that has been little explored is to employ computational modeling to evaluate different bio-compatible osmotic agents replacing glucose to avoid the adverse effects of glucose and glucose by-products in PD patients. Recent advances in modeling includes using PD models to create virtual clinical trials and personalize treatments specific to the patient with the help of their clinicians.

Virtual Patients

The interest in virtual patients is growing, as we have seen with PBPK (physiologically based pharmacokinetic) and PKPD (pharmacokinetic and pharmacodynamic) modeling studies becoming mandatory in drug studies [138,139,140]. Similarly, *in silico* modeling could become essential to medical device development. To realize this, we need digital patient twins. Enabling the use of a virtual platform to test and develop medical devices, would reduce risk and regulatory burden. The FDA also has directed funds towards the establishment of computational modeling as a regulatory tool [141]. A growing virtual database (including patients and animals) could mean that with a computational model, we could identify the risk groups and drug side effects, reduce animal testing, and establish safe protocols.

Complexity of PD devices

Currently, there are several CFPD devices under development using continuous sorbent-based dialysate regeneration (preclinical or clinical developmental phase) [142,143]. To realize these devices in mathematical terms, future work needs to focus on adding flow through a sorbent chamber. There needs to be an evaluation of dead volume- and recirculation-related loss of efficiency in the system due to application of rapid flow cycling via a single lumen catheter. Considering all the potential

parameter settings, which likely influence each other, investigating all parameter combinations is very time consuming, requiring large clinical trials, with many resources and tremendous planning [144]. Computational modeling can help in rapid optimization and avoid unnecessary scenario testing through careful calibration and validation.

Personalization

Other problems with clinical trials include the lack of randomization of patients (inclusivity in terms of sex, age, etc.), difficulty in studying long term effects (due to patient drop out e.g., due to kidney transplantation), lack of blinding, the learning curve (an already existing system may be easier to handle), and general reluctance (by both doctors and patients) to try new technologies [29]. Chronic kidney disease patients also use various medications, which may interfere with the efficiency of the PD session. With mathematical modeling, we can optimize PD treatments [56,145] and conduct virtual PD trials with an inclusive patient spread (age, sex, stage of renal disease, transport parameters, intra-abdominal volume, etc.) and study the short- and long-term effects of different modes of PD. Moreover, PD prescription models such as PatientOnLine [34,146] and PD ADEQUEST [147,148], developed to optimize and personalize PD prescription, have also been validated in multicentre studies. However, the focus of these prescription models is on optimizing the dialysis dose and ultrafiltration and not on patient quality of life. Incorporation of more patient specific factors [149–151] into the model may further personalize PD prescription and contribute to patient well-being.

8. Conclusions

In silico modeling is a powerful tool that can be used to understand gaps in knowledge of both new and old PD devices and facilitates their quick and efficient transition from *in vitro* to *in vivo* to patient care. In this review, we looked at the different modeling approaches explored through the years to model PD and the essential components in a PD compartmental model. We are optimistic that a joint effort of computational modelers and clinicians can help in the technical improvement of PD technology and in personalizing PD treatment to ensure a higher quality of life for patients.

Use of AI tools declaration

The authors declare they have not used Artificial Intelligence (AI) tools in the creation of this article.

Acknowledgements

This work is supported by the partners of Regenerative Medicine Crossing Borders (RegMedXB), a public-private partnership that uses regenerative medicine strategies to cure common chronic diseases, by the Dutch Kidney Foundation and Dutch Ministry of Economic Affairs by means of the PPP Allowance made available by the Top Sector Life Sciences & Health to stimulate public-private partnerships (DKF project code PPS08), by a grant from the Dutch Kidney Foundation (22OK1018) and by the European Union (CORDIAL, Horizon 2020 research and innovation program, grant agreement no. 945207).

Conflict of interest

The authors declare that there is no conflict of interest.

Acronyms

ACE: Angiotensin-Converting Enzyme
APD: Automated Peritoneal Dialysis
AQP1: Aquaporin-1
CAPD: Continuous Ambulatory Peritoneal Dialysis
CFPD: Continuous Flow Peritoneal Dialysis
CCPD: Continuous Cycling Peritoneal Dialysis
CT: Computed Tomography
ESKD: End-Stage Kidney Disease
HD: Hemodialysis
IPV: Intraperitoneal Volume
MTAC: Mass Transfer Area Coefficients
OCG: Osmotic Conductance to Glucose
ODE: Ordinary Differential Equation
PDE: Partial Differential Equation
PD: Peritoneal Dialysis
PK: Pharmacokinetic Model
SAPD: Standard Automated Peritoneal Dialysis
SPA: Standard Peritoneal Assessment
TPM: Three-Pore Model
UF: Ultrafiltration Volume
UFR: Ultrafiltration Rate

Glossary

A = fitting constant for exponential decrease of UF over time (dimensionless)
af = Fraction of peritoneal membrane in contact with fluid (dimensionless); $af = 16.18 * \frac{1-e^{-0.00077*V}}{13.3187}$ [78]
c_{D} = dialysate solute concentration (mmol/l or mmol/m^3), proteins are displayed in g/L or g/dL.
c_{drain} = drain solute concentration (mmol/l)
c_{p} = peripheral vein plasma water solute concentration (mmol/l), proteins are displayed in g/L or g/dL.
$\boldsymbol{c}$ = intramembrane solute concentration (mmol/l)
D = diffusion coefficient (dimensionless)
f = function of Pe (dimensionless)
fct = equilibrium c_p/c_D (dimensionless)
J_{drain} = drain flow rate (l/min)
J_{fill} = fill flow rate (l/min)
J_{v} = volume flux (l/min)
J_{s} = solute flux (mmol/min)

K = permeability coefficient (dimensionless)
L = lymphatic flow (l/min)
L_p = hydraulic conductivity (l/(min.cm^2.mmHg))
$MTAC$ = mass transfer area coefficients (ml/min or m^3/min)
P = hydrostatic pressure (mmHg)
Pe = Peclet number (dimensionless) to determine the importance of convection over diffusion
r = retardation factor (dimensionless)
S = peritoneal surface area (m^2)
$SiCo$ = sieving coefficient (dimensionless)
t = time of session (hr)
UFR = ultrafiltration rate (l/min)
V = intraperitoneal volume (l)
V_r = residual volume (l)
V_{fill} = initial fill volume (l)
V_{drain} = drain volume (l)
W = body weight (kg)

Greek symbols

α = contribution to ultrafiltration coefficient (dimensionless); for ultrasmall pores α_C = 0.02, small pores α_S = 0.9 and for large pores α_L= 0.08
β = time constant for exponential decrease of UF over time (dimensionless)
λ = solute radius/membrane pore radius (dimensionless)
σ = reflection coefficient (dimensionless); calculated for different solutes.
π = oncotic pressure (mmHg)
Φ = equilibrium partition coefficient (dimensionless)
τ = tortuosity factor (dimensionless)

Subscripts

glu = glucose
t = at time t
$fill$ = filling the peritoneal cavity at time 0 (static dwell) or during the session (CFPD, APD)
$drain$ = drain of the peritoneal cavity after (static dwell) or during the dwell (CFPD, APD)
s = solute flux
v = volume flux
C = ultrasmall pores
S = small pores
L = large pores
r = residual

References

1. K. J. Jager, C. Kovesdy, R. Langham, M. Rosenberg, V. Jha, C. Zoccali, A single number for advocacy and communication—worldwide more than 850 million individuals have kidney diseases, *Nephrol. Dial. Transplant.*, **34** (2019), 1803–1805. https://doi.org/10.1093/ndt/gfz174
2. *Fresenius Medical Care Annual Report*, (2021), 39–40.
3. M. Bonomini, V. Zammit, J. C. Divino-Filho, S. J. Davies, L. Di Liberato, A. Arduini, et al., The osmo-metabolic approach: a novel and tantalizing glucose-sparing strategy in peritoneal dialysis, *J. Nephrol.*, **34** (2021), 503–519. https://doi.org/10.1007/s40620-020-00804-2
4. P. Freida, M. Galach, J. C. D. Filho, A. Werynski, B. Lindholm, Combination of crystalloid (glucose) and colloid (icodextrin) osmotic agents markedly enhances peritoneal fluid and solute transport during the long PD dwell, *Perit. Dial. Int.*, **27** (2007), 267–276. https://doi.org/10.1177/089686080702700311
5. K. Nishimura, Y. Kamiya, K. Miyamoto, S. Nomura, T. Horiuchi, Molecular weight of polydisperse icodextrin effects its oncotic contribution to water transport, *J. Artif. Organs*, **11** (2008), 165–169. https://doi.org/10.1007/s10047-008-0423-6
6. J. Stachowska-Pietka, J. Waniewski, A. Olszowska, E. Garcia-Lopez, J. Yan, Q. Yao, et al., Can one long peritoneal dwell with icodextrin replace two short dwells with glucose?, *Front. Physiol.*, **15** (2024). https://doi.org/10.3389/fphys.2024.1339762
7. B. Rippe, G. Stelin, B. Haraldsson, Computer simulations of peritoneal fluid transport in CAPD, *Kidney Int.*, **40** (1991), 315–325. https://doi.org/10.1038/ki.1991.216
8. R. P. Popovich, J. W. Moncrief, K. D. Nolph, A. J. Ghods, Z. J. Twardowski, W. K. Pyle, Continuous ambulatory peritoneal dialysis, *Ann. Intern. Med.*, **88** (1978), 449–456. https://doi.org/10.7326/0003-4819-88-4-449
9. T. A. Golper, R. Chaudhry, Automated cyclers used in peritoneal dialysis: technical aspects for the clinician, *Med. Devices: Evidence Res.*, (2015), 95. https://doi.org/10.2147/mder.s51189
10. B. Marrón, C. Remón, M. Pérez-Fontán, P. Quirós, A. Ortíz, Benefits of preserving residual renal function in peritoneal dialysis, *Kidney Int.*, **73** (2008), S42–S51. https://doi.org/10.1038/sj.ki.5002600
11. B. G. Jaar, L. C. Plantinga, D. C. Crews, N. E. Fink, N. Hebah, J. Coresh, et al., Timing, causes, predictors and prognosis of switching from peritoneal dialysis to hemodialysis: A prospective study, *BMC Nephrol.*, **10** (2009), 3. https://doi.org/10.1186/1471-2369-10-3
12. A. A. Bonenkamp, A. V. E. V. Der Sluijs, F. W. Dekker, D. G. Struijk, C. W. H. De Fijter, Y. M. Vermeeren, et al., Technique failure in peritoneal dialysis: Modifiable causes and patient-specific risk factors, *Perit. Dial. Int.*, (2022), 08968608221077461. https://doi.org/10.1177/08968608221077461
13. A. Van Eck Van Der Sluijs, A. A. Bonenkamp, F. W. Dekker, A. C. Abrahams, B. C. Van Jaarsveld, A. C. Abrahams, et al., Dutch nOcturnal and hoME dialysis Study To Improve Clinical Outcomes (DOMESTICO): rationale and design, *BMC Nephrol.*, **20** (2019), 361. https://doi.org/10.1186/s12882-019-1526-4
14. Nefrovisie,www.nefrovisie.nl
15. T. T. Jansz, M. Noordzij, A. Kramer, E. Laruelle, C. Couchoud, F. Collart, et al., Survival of patients treated with extended-hours haemodialysis in Europe: an analysis of the ERA-EDTA Registry, *Nephrol. Dial. Transplant.*, **35** (2020), 488–495. https://doi.org/10.1093/ndt/gfz208

16. A. W. Y. Yu, K. F. Chau, Y. W. Ho, P. K. T. Li, Development of the "peritoneal dialysis first" model in Hong Kong, *Perit. Dial. Int.*, **27** (2007), 53–55. https://doi.org/10.1177/089686080702702s09
17. C. Ronco, R. Amerling, Continuous flow peritoneal dialysis: current state-of-the-art and obstacles to further development, *Contrib. Nephrol.*, **150** (2006), 310–320. https://doi.org/10.1159/000093625
18. R. Amerling, J. F. Winchester, C. Ronco, Continuous flow peritoneal dialysis: update 2012, *Contrib. Nephrol.*, **178** (2012), 205–215. https://doi.org/10.1159/000337854
19. M. K. Van Gelder, J. C. De Vries, F. Simonis, A. S. Monninkhof, D. H. M. Hazenbrink, G. Ligabue, et al., Evaluation of a system for sorbent-assisted peritoneal dialysis in a uremic pig model, *Physiol. Rep.*, **8** (2020), e14593. https://doi.org/10.14814/phy2.14593
20. M. K. Van Gelder, G. Ligabue, S. Giovanella, E. Bianchini, F. Simonis, D. H. M. Hazenbrink, et al., In vitro efficacy and safety of a system for sorbent-assisted peritoneal dialysis, *Am. J. Physiol. Renal. Physiol.*, **319** (2020), F162–F170. https://doi.org/10.1152/ajprenal.00079.2020
21. K. Gerritsen, WEAKID - Clinical validation of miniature wearable dialysis machine - H2020, *Impact*, **2018** (2018), 55–57. https://doi.org/10.21820/23987073.2018.3.55
22. R. Herzog, M. Bartosova, S. Tarantino, A. Wagner, M. Unterwurzacher, J. M. Sacnun, et al., Peritoneal dialysis fluid supplementation with alanyl-glutamine attenuates conventional dialysis fluid-mediated endothelial cell injury by restoring perturbed cytoprotective responses, *Biomolecules*, **10** (2020). https://doi.org/10.3390/biom10121678
23. P. Freida, M. Wilkie, S. Jenkins, F. Dallas, B. Issad, The contribution of combined crystalloid and colloid osmosis to fluid and sodium management in peritoneal dialysis, *Kidney Int.*, **73** (2008), S102–S111. https://doi.org/10.1038/sj.ki.5002610
24. S. Jenkins, M. Wilkie, Mixing osmotic agents–two different approaches, *Perit. Dial. Int.*, **27** (2007), 245–250. https://doi.org/10.1177/089686080702700306
25. R. Amerling, C. Ronco, N. W. Levin, Continuous-flow peritoneal dialysis, *Perit. Dial. Int.*, **20** (2000), 172–177. https://doi.org/10.1177/089686080002002S32
26. J. A. Diaz-Buxo, Evolution of continuous flow peritoneal dialysis and the current state of the art, *Semin. Dial.*, **14** (2001), 373–377. https://doi.org/10.1046/j.1525-139X.2001.00097.x
27. J. Winchester, R. Amerling, N. Harbord, V. Capponi, C. Ronco, The potential application of sorbents in peritoneal dialysis, *Contrib. Nephrol.*, **150** (2006), 336–343. https://doi.org/10.1159/000093628
28. M. Roberts, The regenerative dialysis (REDY) sorbent system, *Nephrology*, **4** (1998), 275–278. https://doi.org/https://doi.org/10.1111/j.1440-1797.1998.tb00359.x
29. E. A. M. Neugebauer, A. Rath, S. L. Antoine, M. Eikermann, D. Seidel, C. Koenen, et al., Specific barriers to the conduct of randomised clinical trials on medical devices, *Trials*, **18** (2017), 427. https://doi.org/10.1186/s13063-017-2168-0
30. C. A. Labarrere, A. E. Dabiri, G. S. Kassab, Thrombogenic and inflammatory reactions to biomaterials in medical devices, *Front. Bioeng. Biotech.*, **8** (2020). https://doi.org/10.3389/fbioe.2020.00123
31. M. Zilberman, A. Malka, Drug controlled release from structured bioresorbable films used in medical devices—A mathematical model, *J. Biomed. Mater. Res. B Appl. Biomater*, **89B** (2009), 155–164. https://doi.org/10.1002/jbm.b.31200

32. B. Ercan, D. Khang, J. Carpenter, T. J. Webster, Using mathematical models to understand the effect of nanoscale roughness on protein adsorption for improving medical devices, *Int J Nanomedicine*, **8 Suppl 1** (2013), 75–81. https://doi.org/10.2147/IJN.S47286
33. Y. Wang, Y. Zou, X. Chen, J. Zhu, C. Xiang, H. Jia, et al., Identification of the appropriate fixation site to avoid peritoneal catheter migration based on a mechanical analysis, *Ren. Fail.*, **39** (2017), 400–405. https://doi.org/10.1080/0886022X.2017.1291433
34. E. G. Galli, C. Taietti, M. Borghi, Personalization of automated peritoneal dialysis treatment using a computer modeling system, *Adv. Perit. Dial.*, **27** (2011), 90–96.
35. J. W. Yates, R. O. Jones, M. Walker, S. A. Cheung, Structural identifiability and indistinguishability of compartmental models, *Expert Opin. Drug Metab. Toxicol.*, **5** (2009), 295–302. https://doi.org/10.1517/17425250902773426
36. J. King, K. S. Eroumé, R. Truckenmüller, S. Giselbrecht, A. E. Cowan, L. Loew, et al., Ten steps to investigate a cellular system with mathematical modeling, *PLoS Comput. Biol.*, **17** (2021), e1008921. https://doi.org/10.1371/journal.pcbi.1008921
37. R. F. Brown, Compartmental system analysis: State of the art, *IEEE Trans. Biomed. Eng.*, **BME-27** (1980), 1–11. https://doi.org/10.1109/TBME.1980.326685
38. C. M. Öberg, G. Martuseviciene, Computer simulations of continuous flow peritoneal dialysis using the 3-pore model—a first experience, *Perit. Dial. Int.*, **39** (2019), 236–242. https://doi.org/10.3747/pdi.2018.00225
39. M. F. Flessner, R. L. Dedrick, J. S. Schultz, A distributed model of peritoneal-plasma transport: analysis of experimental data in the rat, *Am. J. Physiol. Renal. Physiol.*, **248** (1985), F413–F424. https://doi.org/10.1152/ajprenal.1985.248.3.F413
40. M. P. Hiatt, W. K. Pyle, J. W. Moncrief, R. P. Popovich, A comparison of the relative efficacy of CAPD and hernodialysis in the control of solute concentration, *Artif. Organs*, **4** (1980), 37–43. https://doi.org/10.1111/j.1525-1594.1980.tb03899.x
41. R. J. Kallen, A method for approximating the efficacy of peritoneal dialysis for uremia, *Am. J. Dis. Child.*, **111** (1966), 156–160. https://doi.org/10.1001/archpedi.1966.02090050088005
42. L. W. Henderson, K. D. Nolph, Altered permeability of the peritoneal membrane after using hypertonic peritoneal dialysis fluid, *J. Clin. Invest.*, **48** (1969), 992–1001. https://doi.org/10.1172/jci106080
43. K. D. Nolph, M. I. Sorkin, H. Moore, Autoregulation of sodium and potassium removal during continuous ambulatory peritoneal dialysis, *ASAIO J.*, **26** (1980), 334–338.
44. D. J. Ahearn, K. D. Nolph, Controlled sodium removal with peritoneal dialysis, *ASAIO J.*, **18** (1972), 423–428.
45. V. Moor, R. Wagner, M. Sayer, M. Petsch, S. Rueb, H. U. Häring, et al., Routine monitoring of sodium and phosphorus removal in peritoneal dialysis (PD) patients treated with continuous ambulatory PD (CAPD), automated PD (APD) or combined CAPD + APD, *Kidney Blood Press. Res.*, **42** (2017), 257–266. https://doi.org/10.1159/000477422
46. S. Borrelli, V. La Milia, L. De Nicola, G. Cabiddu, R. Russo, M. Provenzano, et al., Sodium removal by peritoneal dialysis: a systematic review and meta-analysis, *J. Nephrol.*, **32** (2019), 231–239. https://doi.org/10.1007/s40620-018-0507-1
47. K. D. Nolph, F. N. Miller, W. K. Pyle, R. P. Popovich, M. I. Sorkin, An hypothesis to explain the ultrafiltration characteristics of peritoneal dialysis, *Kidney Int.*, **20** (1981), 543–548. https://doi.org/10.1038/ki.1981.175

48. G. M. Preston, T. P. Carroll, W. B. Guggino, P. Agre, Appearance of water channels in Xenopus Oocytes expressing red cell CHIP28 protein, *Science*, **256** (1992), 385–387. https://doi.org/10.1126/science.256.5055.385
49. B. Yang, H. G. Folkesson, J. Yang, M. A. Matthay, T. Ma, A. S. Verkman, Reduced osmotic water permeability of the peritoneal barrier in aquaporin-1 knockout mice, *Am. J. Physiol. Cell. Physiol.*, **276** (1999), C76–C81. https://doi.org/10.1152/ajpcell.1999.276.1.C76
50. D. Venturoli, B. Rippe, Transport asymmetry in peritoneal dialysis: application of a serial heteroporous peritoneal membrane model, *Am. J. Physiol. Renal. Physiol.*, **280** (2001), F599–F606. https://doi.org/10.1152/ajprenal.2001.280.4.F599
51. P. Joffe, J. H. Henriksen, Bidirectional peritoneal transport of albumin in continuous ambulatory peritoneal dialysis, *Nephrol. Dial. Transplant.*, **10** (1995), 1725–1732. https://doi.org/10.1093/ndt/10.9.1725
52. K. Kalantar-Zadeh, D. L. Regidor, C. P. Kovesdy, D. Van Wyck, S. Bunnapradist, T. B. Horwich, et al., Fluid retention is associated with cardiovascular mortality in patients undergoing long-term hemodialysis, *Circulation*, **119** (2009), 671–679. https://doi.org/10.1161/circulationaha.108.807362
53. E. H. Starling, On the absorption of fluids from the connective tissue spaces, *J. Phys.*, **19** (1896), 312–326. https://doi.org/10.1113/jphysiol.1896.sp000596
54. A. Katchalsky, O. Kedem, Thermodynamics of flow processes in biological systems, *Biophys. J.*, **2** (1962), 53–78. https://doi.org/10.1016/s0006-3495(62)86948-3
55. R. Khanna, R. Mactier, Role of lymphatics in peritoneal dialysis, *Blood Purif.*, **10** (1992), 163–172. https://doi.org/10.1159/000170043
56. C. M. Öberg, B. Rippe, Optimizing automated peritoneal dialysis using an extended 3-pore model, *Kidney. Int. Rep.*, **2** (2017), 943–951. https://doi.org/10.1016/j.ekir.2017.04.010
57. Z. J. T. Karl, O. N. R. Khanna, B. F. P. Leonor, P. Ryan, H. L. Moore, M. P. Nielsen, Peritoneal equilibration test, *Perit. Dial. Int.*, **7** (1987), 138–148. https://doi.org/10.1177/089686088700700306
58. A. L. Babb, P. J. Johansen, M. J. Strand, H. Tenckhoff, B. H. Scribner, Bi-directional permeability of the human peritoneum to middle molecules, *Proc. Eur. Dial. Transplant. Assoc.*, (1973), 247–262.
59. A. L. Imholz, G. C. Koomen, D. G. Struijk, L. Arisz, R. T. Krediet, Residual volume measurements in CAPD patients with exogenous and endogenous solutes, in *Conference Proceedings from Advances in Peritoneal Dialysis*, (1992), 33–38.
60. E. Lindholm, G. Martus, C. M. Öberg, K. Bergling, Determining the residual volume in peritoneal dialysis using low molecular weight markers, *Perit. Dial. Int.*, (2024), 08968608241260024. https://doi.org/10.1177/08968608241260024
61. G. Martus, K. Bergling, O. Simonsen, E. Goffin, J. Morelle, C. M. Öberg, Novel method for osmotic conductance to glucose in peritoneal dialysis, *Kidney. Int. Rep.*, **5** (2020), 1974–1981. https://doi.org/10.1016/j.ekir.2020.09.003
62. P. Y. Durand, J. Chanliau, J. Gamberoni, D. Hestin, M. Kessler, Intraperitoneal hydrostatic pressure and ultrafiltration volume in CAPD, in *Conference Proceedings from Advances in Peritoneal Dialysis*, (1993), 46–48.

63. Z. J. Twardowski, B. F. Prowant, K. D. Nolph, A. J. Martinez, L. M. Lampton, High volume, low frequency continuous ambulatory peritoneal dialysis, *Kidney Int.*, **23** (1983), 64–70. https://doi.org/10.1038/ki.1983.12
64. E. R. Zakaria, B. Rippe, Intraperitoneal fluid volume changes during peritoneal dialysis in the rat: indicator dilution vs. volumetric measurements, *Blood Purif.*, **13** (1995), 255–270. https://doi.org/10.1159/000170209
65. A. H. Pust, J. K. Leypoldt, R. P. Frigon, L. W. Henderson, Peritoneal dialysate volume determined by indicator dilution measurements, *Kidney Int.*, **33** (1988), 64–70. https://doi.org/10.1038/ki.1988.10
66. D. Faict, N. Lameire, D. Kesteloot, F. Peluso, Evaluation of peritoneal dialysis solutions with amino acids and glycerol in a rat model, *Nephrol. Dial. Transplant.*, **6** (1991), 120–124. https://doi.org/10.1093/ndt/6.2.120
67. T. W. Chen, R. Khanna, H. Moore, Z. J. Twardowski, K. D. Nolph, Sieving and reflection coefficients for sodium salts and glucose during peritoneal dialysis in rats, *J. Am. Soc. Nephrol.*, **2** (1991), 1092. https://doi.org/10.1681/ASN.V261092
68. F. E. Curry, C. C. Michel, J. C. Mason, Osmotic reflextion coefficients of capillary walls to low molecular weight hydrophilic solutes measured in single perfused capillaries of the frog mesentery, *J. Physiol.*, **261** (1976), 319–336. https://doi.org/10.1113/jphysiol.1976.sp011561
69. R. Drake, E. Davis, A corrected equation for the calculation of reflection coefficients, *Microvasc. Res.*, **15** (1978), 259.
70. E. A. Mason, R. P. Wendt, E. H. Bresler, Similarity relations (dimensional analysis) for membrane transport, *J. Membr. Sci.*, **6** (1980), 283–298. https://doi.org/10.1016/S0376-7388(00)82170-5
71. J. L. Anderson, Configurational effect on the reflection coefficient for rigid solutes in capillary pores, *J. Theor. Biol.*, **90** (1981), 405–426. https://doi.org/10.1016/0022-5193(81)90321-0
72. V. La Milia, M. Limardo, G. Virga, M. Crepaldi, F. Locatelli, Simultaneous measurement of peritoneal glucose and free water osmotic conductances, *Kidney Int.*, **72** (2007), 643–650. https://doi.org/10.1038/sj.ki.5002405
73. A. L. Clause, M. Keddar, R. Crott, T. Darius, C. Fillee, E. Goffin, et al., A large intraperitoneal residual volume hampers adequate volumetric assessment of osmotic conductance to glucose, *Perit. Dial. Int.*, **38** (2018), 356–362. https://doi.org/10.3747/pdi.2017.00219
74. C. M. Öberg, B. Rippe, A distributed two-pore model: theoretical implications and practical application to the glomerular sieving of Ficoll, *Am. J. Physiol. Renal. Physiol.*, **306** (2014), F844–F854. https://doi.org/10.1152/ajprenal.00366.2013
75. B. Rippe, A three-pore model of peritoneal transport, *Perit. Dial. Int.*, **13** (1993), 35–38. https://doi.org/10.1177/089686089301302S09
76. B. Rippe, G. Stelin, Simulations of peritoneal solute transport during CAPD. Application of two-pore formalism, *Kidney Int.*, **35** (1989), 1234–1244. https://doi.org/10.1038/ki.1989.115
77. P. Keshaviah, P. F. Emerson, E. F. Vonesh, J. C. Brandes, Relationship between body size, fill volume, and mass transfer area coefficient in peritoneal dialysis, *J. Am. Soc. Nephrol.*, **4** (1994), 1820. https://doi.org/10.1681/ASN.V4101820
78. C. M. Öberg, B. Rippe, Is adapted APD theoretically more efficient than conventional APD?, *Perit. Dial. Int.*, **37** (2017), 212–217. https://doi.org/10.3747/pdi.2015.00144

79. E. Breton, P. Choquet, L. Bergua, M. Barthelmebs, B. Haraldsson, J. J. Helwig, et al., In vivo peritoneal surface area measurement in rats by micro-computed tomography (μCT), *Perit. Dial. Int.*, **28** (2008), 188–194. https://doi.org/10.1177/089686080802800216
80. A. Chagnac, P. Herskovitz, T. Weinstein, S. Elyashiv, J. Hirsh, I. Hammel, et al., The peritoneal membrane in peritoneal dialysis patients, *J. Am. Soc. Nephrol.*, **10** (1999), 342. https://doi.org/10.1681/ASN.V102342
81. M. Fischbach, A. C. Michallat, G. Zollner, C. Dheu, M. Barthelmebs, J. J. Helwig, et al. Measurement by magnetic resonance imaging of the peritoneal membrane in contact with dialysate in rats, *Adv. Perit. Dial.*, **21** (2005), 17.
82. A. Chagnac, P. Herskovitz, Y. Ori, T. Weinstein, J. Hirsh, M. Katz, et al., Effect of increased dialysate volume on peritoneal surface area among peritoneal dialysis patients, *J. Am. Soc. Nephrol.*, **13** (2002), 2554. https://doi.org/10.1097/01.ASN.0000026492.83560.81
83. M. F. Flessner, J. Lofthouse, E. R. Zakaria, Improving contact area between the peritoneum and intraperitoneal therapeutic solutions, *J. Am. Soc. Nephrol.*, **12** (2001), 807. https://doi.org/10.1681/ASN.V124807
84. M. Y. Jaffrin, R. A. Odell, P. C. Farrell, A model of ultrafiltration and glucose mass transfer kinetics in peritoneal dialysis, *Artif. Organs*, **11** (1987), 198–207. https://doi.org/10.1111/j.1525-1594.1987.tb02660.x
85. E. F. Vonesh, M. J. Lysaght, J. Moran, P. Farrell, Kinetic modeling as a prescription aid in peritoneal dialysis, *Blood Purif.*, **9** (1991), 246–270. https://doi.org/10.1159/000170024
86. J. Graff, S. Fugleberg, P. Joffe, J. Brahm, N. Fogh-Andersen, An evaluation of twelve nested models of transperitoneal transport of urea: the one-compartment assumption is valid, *Scand. J. Clin. Lab. Invest.*, **55** (1995), 331–339. https://doi.org/10.3109/00365519509104971
87. J. Graff, S. Fugleberg, P. Joffe, N. Fogh-Andersen, Parameter estimation in six numeric models of transperitoneal transport of glucose, *ASAIO J.*, **40** (1994), 1005–1011.
88. J. Graff, S. Fugleberg, P. Joffe, J. Brahm, N. Fogh - Andersen, Parameter estimation in six numerical models of transperitoneal transport of potassium in patients undergoing peritoneal dialysis, *Clin. Physiol.*, **15** (1995), 185–197. https://doi.org/10.1111/j.1475-097x.1995.tb00510.x
89. S. Fugleberg, J. Graff, P. Joffe, H. Løkkegaard, B. Feldt - Rasmussen, N. Fogh - Andersen, et al., Transperitoneal transport of creatinine. A comparison of kinetic models, *Clin. Physiol.*, **14** (1994), 443–457. https://doi.org/10.1111/j.1475-097x.1994.tb00403.x
90. J. Graff, S. Fugleberg, J. Brahm, N. Fogh - Andersen, Transperitoneal transport of sodium during hypertonic peritoneal dialysis, *Clin. Physiol.*, **16** (1996), 31–39. https://doi.org/10.1111/j.1475-097x.1996.tb00554.x
91. J. Graff, S. Fugleberg, J. Brahm, N. Fogh - Andersen, The transport of phosphate between the plasma and dialysate compartments in peritoneal dialysis is influenced by an electric potential difference, *Clin. Physiol.*, **16** (1996), 291–300. https://doi.org/10.1111/j.1475-097x.1996.tb00575.x

92. J. Waniewski, A. Werynski, O. Heimbürger, B. Lindholm, Simple models for description of small-solute transport in peritoneal dialysis, *Blood Purif.*, **9** (1991), 129–141. https://doi.org/10.1159/000170009
93. R. T. Krediet, L. Arisz, Fluid and solute transport across the peritoneum during continuous ambulatory peritoneal dialysis (CAPD), *Perit. Dial. Int.*, **9** (1989), 15–25. https://doi.org/10.1177/089686088900900104
94. D. H. Randerson, Continuous ambulatory peritoneal dialysis-A critical appraisal, Australia: The University of South Wales, 1980.
95. R. T. Krediet, D. G. Struijk, E. W. Boeschoten, F. J. Hoek, L. Arisz, Measurement of intraperitoneal fluid kinetics in CAPD patients by means of autologous haemoglobin, *Neth. J. Med.*, **33** (1988), 281–290.
96. F. A. Gotch, Kinetic modeling of continuous flow peritoneal dialysis, *Semin. Dial.*, **14** (2001), 378–383. https://doi.org/10.1046/j.1525-139x.2001.00096.x
97. C. S. Patlak, D. A. Goldstein, J. F. Hoffman, The flow of solute and solvent across a two-membrane system, *J. Theor. Biol.*, **5** (1963), 426–442. https://doi.org/10.1016/0022-5193(63)90088-2
98. J. K. Leypoldt, A. H. Pust, R. P. Frigon, L. W. Henderson, Dialysate volume measurements required for determining peritoneal solute transport, *Kidney Int.*, **34** (1988), 254–261. https://doi.org/10.1038/ki.1988.173
99. F. Villarroel, Kinetics of intermittent and continuous peritoneal dialysis, *J. Dial.*, **1** (1977), 333–347. https://doi.org/10.3109/08860227709038424
100. L. J. Garred, B. Canaud, P. C. Farrell, A simple kinetic model for assessing peritoneal mass transfer in chronic ambulatory peritoneal dialysis, *ASAIO J.*, **6** (1983), 131–137.
101. J. Waniewski, J. Stachowska-Pietka, B. Lindholm, On the change of transport parameters with dwell time during peritoneal dialysis, *Perit. Dial. Int.*, **41** (2020), 404–412. https://doi.org/10.1177/0896860820971519
102. J. Stachowska-Pietka, J. Waniewski, M. F. Flessner, B. Lindholm, Distributed model of peritoneal fluid absorption, *Am. J. Physiol. Heart. Circ. Physiol.*, **291** (2006), H1862–H1874. https://doi.org/10.1152/ajpheart.01320.2005
103. J. Waniewski, J. Stachowska-Pietka, R. Cherniha, B. Lindholm, Swelling of peritoneal tissue during peritoneal dialysis: Computational assessment using poroelastic theory, *Nephrol. Dial. Transplant.*, **36** (2021), gfab101.0016. https://doi.org/10.1093/ndt/gfab101.0016
104. R. Cherniha, K. Gozak, J. Waniewski, Exact and numerical solutions of a spatially-distributed mathematical model for fluid and solute transport in peritoneal dialysis, *Symmetry*, **8** (2016). https://doi.org/10.3390/sym8060050
105. R. Cherniha, J. Stachowska-Piętka, J. Waniewski, A mathematical model for fluid-glucose-albumin transport in peritoneal dialysis, *Int. J. Appl. Math. Comput. Sci.*, **24** (2014), 837–851. https://doi.org/doi:10.2478/amcs-2014-0062
106. A. Akonur, C. J. Holmes, J. K. Leypoldt, Predicting the peritoneal absorption of icodextrin in rats and humans including the effect of α–amylase activity in dialysate, *Perit. Dial. Int.*, **35** (2015), 288–296. https://doi.org/10.3747/pdi.2012.00247
107. Z. J. Twardowski, PET—a simpler approach for determining prescriptions for adequate dialysis therapy, in *Conference Proceedings from Advances in Peritoneal Dialysis*, **6** (1990), 186–191.

108. M. M. Pannekeet, A. L. T. Imholz, D. G. Struijk, G. C. M. Koomen, M. J. Langedijk, N. Schouten, et al., The standard peritoneal permeability analysis: A tool for the assessment of peritoneal permeability characteristics in CAPD patients, *Kidney Int.*, **48** (1995), 866–875. https://doi.org/10.1038/ki.1995.363
109. R. T. Krediet, E. W. Boeschoten, F. M. J. Zuyderhoudt, J. Strackee, L. Arisz, Simple assessment of the efficacy of peritoneal transport in continuous ambulatory peritoneal dialysis patients, *Blood Purif.*, **4** (1986), 194–203. https://doi.org/10.1159/000169445
110. G. A. Tanner, Glomerular sieving coefficient of serum albumin in the rat: a two-photon microscopy study, *Am. J. Physiol. Renal. Physiol.*, **296** (2009), F1258–F1265. https://doi.org/10.1152/ajprenal.90638.2008
111. B. Rippe, B. Haraldsson, Transport of macromolecules across microvascular walls: the two-pore theory, *Physiol. Rev.*, **74** (1994), 163–219. https://doi.org/10.1152/physrev.1994.74.1.163
112. J. H. Miller, R. Gipstein, R. Margules, M. Schwartz, M. E. Rubini, Automated peritoneal dialysis: Analysis of several methods of peritoneal dialysis, *ASAIO J.*, **12** (1966), 98–105.
113. R. A. Mactier, R. Khanna, Z. Twardowski, H. Moore, K. D. Nolph, Contribution of lymphatic absorption to loss of ultrafiltration and solute clearances in continuous ambulatory peritoneal dialysis, *J. Clin. Invest.*, **80** (1987), 1311–1316. https://doi.org/10.1172/jci113207
114. M. F. Flessner, Peritoneal transport physiology: insights from basic research, *J. Am. Soc. Nephrol.*, **2** (1991), 122–135. https://doi.org/10.1681/asn.v22122
115. M. F. Flessner, R. L. Dedrick, J. S. Schultz, A distributed model of peritoneal-plasma transport: theoretical considerations, *Am. J. Physiol. Regul. Integr. Comp. Physiol.*, **246** (1984), R597–R607. https://doi.org/10.1152/ajpregu.1984.246.4.R597
116. B. Rippe, D. Venturoli, O. Simonsen, J. De Arteaga, Fluid and electrolyte transport across the peritoneal membrane during CAPD according to the three-pore model, *Perit. Dial. Int.*, **24** (2004), 10–27. https://doi.org/10.1177/089686080402400102
117. J. Stachowska-Pietka, J. Waniewski, A. Olszowska, E. Garcia-Lopez, Z. Wankowicz, B. Lindholm, Modelling of icodextrin hydrolysis and kinetics during peritoneal dialysis, *Sci. Rep.*, **13** (2023), 6526. https://doi.org/10.1038/s41598-023-33480-w
118. J. Waniewski, A. Werynski, O. Heimbürger, B. Lindholm, Simple membrane models for peritoneal dialysis evaluation of diffusive and convective solute transport, *ASAIO J.*, **38** (1992), 788–8796.
119. A. Akonur, Y. C. Lo, B. Cizman. A mathematical model to optimize the drain phase in gravity-based peritoneal dialysis systems, *Adv. Perit.Dial.*, **26** (2010).
120. K. J. Lee, D. A. Shin, H. S. Lee, J. C. Lee, Computer simulations of steady concentration peritoneal dialysis, *Perit. Dial. Int.*, **40** (2020), 76–83. https://doi.org/10.1177/0896860819878635
121. M. B. Wolf, Mechanisms of peritoneal acid-base kinetics during peritoneal dialysis: a mathematical model study, *ASAIO J.*, **67** (2021). https://doi.org/10.1097/MAT.0000000000001300
122. J. M. Hartinger, D. Michaličková, E. Dvořáčková, K. Hronová, E. H. J. Krekels, B. Szonowská, et al., Intraperitoneally administered vancomycin in patients with peritoneal dialysis-associated peritonitis: Population pharmacokinetics and dosing implications, *Pharmaceutics*, **15** (2023). https://doi.org/10.3390/pharmaceutics15051394
123. I. J. Torres, C. L. Litterst, A. M. Guarino, Transport of model compounds across the peritoneal membrane in the rat, *Pharmacology*, **17** (1978), 330–340. https://doi.org/10.1159/000136874

124. K. Hirano, C. A. Hunt, Lymphatic transport of liposome-encapsulated agents: effects of liposome size following intraperitoneal administration, *J. Pharm. Sci.*, **74** (1985), 915–921. https://doi.org/10.1002/jps.2600740902
125. A. Sarfarazi, G. Lee, S. A. Mirjalili, A. R. J. Phillips, J. A. Windsor, N. L. Trevaskis, Therapeutic delivery to the peritoneal lymphatics: Current understanding, potential treatment benefits and future prospects, *Int. J. Pharm.*, **567** (2019), 118456. https://doi.org/10.1016/j.ijpharm.2019.118456
126. M. C. Rogge, C. A. Johnson, S. W. Zimmerman, P. G. Welling, Vancomycin disposition during continuous ambulatory peritoneal dialysis: a pharmacokinetic analysis of peritoneal drug transport, *Antimicrob. Agents Chemother.*, **27** (1985), 578–582. https://doi.org/10.1128/AAC.27.4.578
127. E. Nakashima, R. Matsushita, T. Ohshima, A. Tsuji, F. Ichimura, Quantitative relationship between structure and peritoneal membrane transport based on physiological pharmacokinetic concepts for acidic drugs, *Drug. Metab. Dispos.*, **23** (1995), 1220–1224.https://pubmed.ncbi.nlm.nih.gov/8591722/
128. R. L. Dedrick, C. E. Myers, P. M. Bungay, V. T. Devita, Pharmacokinetic rationale for peritoneal drug administration, *Cancer Treat Rep.*, **62** (1978), 1–11. https://pubmed.ncbi.nlm.nih.gov/626987/
129. E. Feder, J. Knapowski, Effects of furosemide and ethacrynic acid on sodium transfer across the parietal peritoneal membrane, *Physiology of Non-Excitable Cells*: Pergamon, (1981), 163–167.
130. I. Kolesnyk, F. W. Dekker, M. Noordzij, S. Le Cessie, D. G. Struijk, R. T. Krediet, Impact of ACE inhibitors and AII receptor blockers on peritoneal membrane transport characteristics in long-term peritoneal dialysis patients, *Perit. Dial. Int.*, **27** (2007), 446–453. https://doi.org/10.1177/089686080702700413
131. R. L. Dedrick, M. F. Flessner, Pharmacokinetic problems in peritoneal drug administration: tissue penetration and surface exposure, *J. Natl. Cancer. Inst.*, **89** (1997), 480–487. https://doi.org/10.1093/jnci/89.7.480
132. P. K. T. Li, K. M. Chow, Y. Cho, S. Fan, A. E. Figueiredo, T. Harris, et al., ISPD peritonitis guideline recommendations: 2022 update on prevention and treatment, *Perit. Dial. Int.*, **42** (2022), 110–153. https://doi.org/10.1177/08968608221080586
133. J. Stachowska-Pietka, J. Waniewski, M. F. Flessner, B. Lindholm, Computer simulations of osmotic ultrafiltration and small-solute transport in peritoneal dialysis: A spatially distributed approach, *Am. J. Physiol. Renal. Physiol.*, **302** (2012), F1331–F1341. https://doi.org/10.1152/ajprenal.00301.2011
134. V. M. E. Paguio, F. Kappel, P. Kotanko, A model of vascular refilling with inflammation, *Math. Biosci.*, **303** (2018), 101–114. https://doi.org/10.1016/j.mbs.2018.06.007
135. K. Bergling, G. Martus, C. M. Öberg, Phloretin improves ultrafiltration and reduces glucose absorption during peritoneal dialysis in rats, *J. Am. Soc. Nephrol.*, **33** (2022). https://doi.org/10.1681/ASN.2022040474
136. S. F. Mousavi, M. M. Sepehri, R. Khasha, S. H. Mousavi, Improving vascular access creation among hemodialysis patients: An agent-based modeling and simulation approach, *Artif. Intell. Med.*, **126** (2022), 102253. https://doi.org/10.1016/j.artmed.2022.102253
137. F. A. Gotch, B. J. Lipps, PACK PD: a urea kinetic modeling computer program for peritoneal dialysis, *Perit. Dial. Int.*, **17** (1997), 126–130. https://doi.org/10.1177/089686089701702S24

138. M. Allison, Reinventing clinical trials, *Nat. Biotechnol.*, **30** (2012), 41–49. https://doi.org/10.1038/nbt.2083
139. D. Alemayehu, R. Hemmings, K. Natarajan, S. Roychoudhury, Perspectives on virtual (remote) clinical trials as the "new normal" to accelerate drug development *Clin. Pharmacol. Ther.*, **111** (2022), 373–381. https://doi.org/10.1002/cpt.2248
140. S. Sinisi, V. Alimguzhin, T. Mancini, E. Tronci, B. Leeners, Complete populations of virtual patients for in silico clinical trials, *Bioinformatics*, **36** (2020), 5465–5472. https://doi.org/10.1093/bioinformatics/btaa1026
141. T. M. Morrison, P. Pathmanathan, M. Adwan, E. Margerrison, Advancing regulatory science with computational modeling for medical devices at the FDA's Office of Science and Engineering Laboratories, *Front. Med.*, **5** (2018), 241.
142. H. Htay, S. K. Gow, M. Jayaballa, E. L. Oei, C. M. Chan, S. Y. Wu, et al., Preliminary safety study of the automated wearable artificial kidney (AWAK) in peritoneal dialysis patients, *Perit. Dial. Int.*, **42** (2022), 394–402. https://doi.org/10.1177/08968608211019232
143. M. K. V. Gelder, J. C. De Vries, F. Simonis, J. A. Joles, M. A. B. Rubio, R. Selgas, et al., Rationale and design of the CORDIAL first-in-human clinical trial: a system for sorbent-assisted continuous flow peritoneal dialysis, *Nephrol. Dial. Transplant.*, **39** (2022), 1637–3022. https://doi.org/10.1093/ndt/gfae069.1637
144. E. S. Izmailova, J. A. Wagner, E. D. Perakslis, Wearable devices in clinical trials: hype and hypothesis, *Clin. Pharmacol. Ther.*, **104** (2018), 42–52. https://doi.org/10.1002/cpt.966
145. A. Foux, N. Galili, O. S. Better, Dynamics of dialysis I. intermittent flow peritoneal dialysis, *Math. Biosci.*, **12** (1971), 147–158. https://doi.org/10.1016/0025-5564(71)90079-4
146. E. Hodzic, S. Rasic, C. Klein, A. Covic, A. Unsal, J. M. G. Cunquero, et al., Clinical validation of a peritoneal dialysis prescription model in the patient on line software, *Artif. Organs*, **40** (2016), 144–152. https://doi.org/10.1111/aor.12526
147. E. F. Vonesh, J. Burkart, S. D. Mcmurray, P. F. Williams, Peritoneal dialysis kinetic modeling: validation in a multicenter clinical study, *Perit. Dial. Int.*, **16** (1996), 471–481. https://doi.org/10.1177/089686089601600509
148. E. F. Vonesh, K. O. Story, W. T. O'neill, A multinational clinical validation study of PD Adequest 2.0, *Perit. Dial. Int.*, **19** (1999), 556–571. https://doi.org/10.1177/089686089901900611
149. R. Yazici, L. Altintepe, I. Guney, M. Yeksan, H. Atalay, S. Turk, et al., Female sexual dysfunction in peritoneal dialysis and hemodialysis patients, *Ren. Fail.*, **31** (2009), 360–364. https://doi.org/10.1080/08860220902883012
150. A. Navaratnarajah, M. Clemenger, J. Mcgrory, N. Hisole, T. Chelapurath, R. W. Corbett, et al., Flexibility in peritoneal dialysis prescription: Impact on technique survival, *Perit. Dial. Int.*, **41** (2021), 49–56. https://doi.org/10.1177/0896860820911521
151. A. González López, Á. Nava Rebollo, B. Andrés Martín, F. Herrera Gómez, H. Santana Zapatero, J. Diego Martín, et al., Degree of adherence and knowledge prior to medication reconciliation in patients on peritoneal dialysis, *Nefrología (English Edition)*, **36** (2016), 459–460. https://doi.org/10.1016/j.nefroe.2016.09.005